DOI: https://doi.org/10.52651/sam.j.2025.1

SCIENCE & MILITARY

No 1 | Volume 20 | 2025

SCIENCE & MILITARY

The rationale for publishing this periodical by the Armed Forces Academy of General Milan Rastislav Štefánik is to enable the authors to publish their articles focused on particular scientific issues in the following areas: Military science, Natural Sciences, Engineering and Technology. Original scientific articles will be published twice a year.

Published by: Armed Forces Academy of General Milan Rastislav Štefánik, Demänová 393, 031 01 Liptovský Mikuláš, Slovak Republic. IČO 37 910 337. Registered No: EV 2061/08. ISSN 1336-8885 (print). ISSN 2453-7632 (online).
DOI: http://doi.org/10.52651/sam.j.2025.1
Printed by: EDIS-Publishing House UNIZA, Univerzitná ul. 8215/1, 010 26 Žilina, Slovak Republic.
Published biannually. The subscription rate for one year is 7,30 €.
The Journal Science & Military is included in following multiple databases: EBSCO. ProQuest Central: PQ Science Journals; PQ Military Collection; PQ Computing; PQ Telecommunications; Illustrata; Forthcoming Technology; Research Database (TRD) full text packages.

Address of the editorial office
Armed Forces Academy of General Milan Rastislav Štefánik, Demänová 393, 031 01 Liptovský Mikuláš, Slovak Republic
Phone: +421-960-423065 E-mail: redakcia@aos.sk, https://www.aos.sk/katedry/science-military

DOI: https://doi.org/10.52651/sam.j.2025.1

SCIENCE & MILITARY

No 1 | Volume 20 | 2025

Dear Readers,

We are pleased to introduce the latest issue of the peer-reviewed journal Science & Military, a journal that aspires to join the prestigious international Scopus database. This objective stems from our long-term efforts to improve the scientific quality, transparency, and visibility of the published papers. To achieve this goal, it is essential to further focus on increasing the visibility and citation rate of individual articles published in Science & Military.

Open Access (OA) plays an important role in this regard as it ensures that all published papers are accessible to the wider expert community without any restrictions. We believe that open-knowledge sharing promotes faster scientific progress, facilitates cross-institutional collaboration, and increases the international impact of scientific and research results. In addition, we would like to emphasise that scientific research in the field of military science is of key importance to modern armed forces and security sectors and can contribute to increasing global security. It should be noted that the outputs published in Science & Military can also be used outside the military environment.

Increasing the journal's citation rate is a joint effort shared between the editorial board and the authors. In this regard, we would like to reach out to you, the scientific community, both in Slovakia and abroad, and invite you to collaborate with us. Your scientific outputs can significantly contribute to enhancing the quality and reputation of Science & Military, which has the potential to be recognised not only nationally but also internationally.

Sharing scientific outputs is not just a formal obligation. It improves the professional profile of researchers, their visibility in the scientific community, and opens doors to cooperation and recognition. We try to pay special attention to doctoral students and early-career researchers, for whom publishing scientific outputs is the first step on the path to professional growth. By publishing in a peer-reviewed scientific journal, they gain valuable experience in formulating scientific arguments, working with resources, methodology, and scientific debates.

We sincerely believe that together we will succeed in increasing the journal's professional credibility and bringing it closer to being included in the prestigious international Scopus database.

Dear readers, let me briefly present the contents of the current issue:

The first among the peer-reviewed articles in this issue is the article titled ***"What is the Exact Load Capacity of the Existing Road Bridges? Example Static Calculation for Military Transport Verified by Test Load"*** *written by Bence Hajós. The paper presents the safety aspects that influence the design of bridges and presents a sample static calculation, a load capacity check of a 36 m span reinforced concrete bridge. This article reviews experimental measurements from a proof-load test.*

The author Robert Rozgonyi wrote the paper titled ***"Operational Use of Multispectral Methods against UAS Effects".*** *This article deals with the methods for effective localization and identification of UAS, particularly through the use of multispectral cameras that operate across different bands of the electromagnetic spectrum. The article also discusses the emerging threat posed by optically tethered drones, which bypass standard jamming techniques.*

The series of articles is closed with the paper titled ***"Tribotechnical Diagnostics – Analysis of Engine Oil Degradation Via Oil Properties of SAE 10W – 30 in Tatra Phoenix During 9 Month of Use"*** *written by Adam Fulek, Vladimír Kadlub and Miroslav Marko. This paper deals with the selected degradation elements in the context of tribodiagnostic measurement. It presents the measurements and interpretation of total additivity levels - particularly useful for evaluating remaining oil performance reserve. The paper also deals with the observation of wear particles and elemental composition changes (Fe, Si, Zn, etc.) over time. It presents the measurements on the SpectroCube, FeroCheck and the electron microscope in more detail.*

In conclusion, I would like to thank you for your continued interest and support, and wish you pleasant, inspiring and interesting reading.

Prof. Dipl. Eng. Marcel HARAKAĽ, PhD.
Chairman of the Editorial Board

Reviewers

LTC Dipl. Eng. Matúš **GREGA**, PhD.
Armed Forces Academy of General Milan Rastislav Štefánik, Liptovský Mikuláš, SK

Prof. Dipl. Eng. Peter **KOTEŠ**, PhD.
University of Žilina, Žilina, SK

Assoc. Prof. Dipl. Eng. Pavel **MAŇAS**, Ph.D.
University of Defence, Brno, CZ

Dipl. Eng. Pavol **MIKUŠ**, PhD.
Alexander Dubček University of Trenčín, Trenčín, SK

Assoc. Prof. Dipl. Eng. Pavol **PECHO**, PhD.
University of Žilina, Žilina, SK

Dipl. Eng. Štepán **PRAVDA**
VSB – Technical University of Ostrava, Ostrava, CZ

DOI: https://doi.org/10.52651/sam.a.2025.1.5-10

WHAT IS THE EXACT LOAD CAPACITY OF THE EXISTING ROAD BRIDGES? EXAMPLE STATIC CALCULATION FOR MILITARY TRANSPORT VERIFIED BY TEST LOAD

Bence HAJÓS

Abstract: When assessing the military load capacity of existing road bridges, safety factors, dynamic factors and other parameters are important basic data. Together they determine the safety level of the bridges. This paper reviews the safety aspects that influence the design of bridges and presents a sample static calculation, a load capacity check of a 36 m span reinforced concrete bridge. A military vehicle weighing 105 tonnes was verified to pass over the bridge with a civilian load capacity of 40 tonnes. This was demonstrated and verified by a test load.

Keywords: military transport, road bridges, load capacity, test load, STANAG 2021, Leopard 2 MBT.

1 INTRODUCTION

Military mobility requires a good road network. The most critical points of the network are bridges. One of the most important issues in managing bridges is the load capacity of the bridge. The question is simple, but the answer is difficult. What is the load capacity of a bridge?

When building a new bridge, the design specifications will tell us what parameters the bridge must meet, what payload it must be able to carry and what level of safety the new structure must be able to provide. The designer's task is simple: to prepare the structural analysis according to the bridge design specification. Therefore, the designer typically does not have to deal with the magnitude of safety and the theoretical basis of safety.

Most road bridges are suitable for normal road traffic without weight restrictions. A case-by-case check of the load capacity is required for vehicles heavier than normal road traffic (above 40 tonnes) [1]. Such vehicles may be civilian vehicles (e.g. transport of transformers or generators) or military vehicles (main battle tanks, transport of heavy equipment). Military traffic may also include wheeled and tracked vehicles. Note that an individual inspection of the existing bridge is also required in cases where the load capacity of the bridge is less than 40 tonnes.

The bridge inspector has more freedom in the examination of overweight vehicles than when designing a new bridge. In such cases, specific safety levels may be applied - in each case with a thorough examination of the circumstances. We present the aspects that can be taken into account to calculate a higher payload capacity for an existing bridge.

For military mobility, the suitability of bridges for the transport of overweight vehicles must be known on a national level, in a network system. The transport of civil oversized vehicles is easier because they are typically used on an ad hoc basis and it is possible to use larger diversions.

This study present an existing road bridge with a civilian load capacity of 40 tonnes (Fig. 1), which was also suitable for a military vehicle weighing 105 tonnes under special conditions. The higher load capacity allowed by the specific static check was demonstrated by a test load and the test load justified our specific calculation.

Fig. 1 View of the selected bridge
Source: Photographed by Benedek Kapin.

There are several international examples of load-bearing capacity testing of existing bridges using test loads. The ŽM 60 type temporary road and railway bridge system developed in Czechoslovakia in the 1980s can be used to construct temporary bridges with spans of 30-90 m. The finite element analysis and proof-load testing of the bridge system were used to determine [2] the normal road, exclusive, heavy road, railway and military load-bearing capacity values in accordance with NATO requirements for different spans. The study is unique in that it specifies load-bearing classes for different types of use. There was only a very small difference between the calculated and measured deflection values of the bridge examined in the study (99 %, 87 %). The study also shows in detail how much higher military load-bearing capacity can be justified if the crossing conditions are tightened [2].

The results of test loads can also be used to determine the load-bearing capacity of existing

bridges. Taking test load results into account increases the reliability of the initial parameters [3].

Test loading is also well suited for assessing the load-bearing capacity of existing railway bridges. The safety factor used for dead weight is 1.20 when checking the geometric parameters and 1.30 without checking the geometric parameters. The safety factor for the payload was taken as 1.40 for bridges less than 30 years old and 1.25 for bridges older than 30 years, depending on the age and remaining service life of the bridge [4].

Load tests are sometimes necessary to determine the actual and correct behaviour of bridge structures [5]. In a study presenting load tests on two road bridges in Slovakia, deflections were calculated using two different models. The more detailed calculation agreed well with the actual measurements (78-99 % and 68-92 %), while the simpler model showed greater deviations (62-123 % and 140-163 %).

2 ELEMENTS OF THE SAFETY

A road bridge is designed to carry vehicles safely. Safety depends on many factors, some of which can be well modelled and calculated on a probabilistic basis, some of which cannot. Therefore, the level of safety of bridges is determined using a semi-probability method.

Safety must compensate for the uncertainty of design, ground investigation, materials, construction, construction control, testing, missing maintenance, structural system, vehicle loading, vehicle frequency, vehicle location, etc. Each country's standard is valid for the conditions in that country. It is understood that each country has a different degree of uncertainty in the above. But there can also be significant differences within a country.

In Hungary, there is a clear separation between the reliability of bridges on the national road network. These bridges are subject to more rigorous monitoring, from the selection of the designer through to construction and inspections. It can be concluded that the reliability of bridges on the national road network is better than that of other (e.g. municipal) bridges in Hungary.

Reliability is influenced by many factors. This includes the age of the bridge, because the uncertainty factors listed above have changed in different eras. It is also possible to identify those structural systems with higher uncertainty than the average bridge (e.g. pilot or experimental structures, poor precast concrete girder type, corrosion sensitive, etc.).

On the basis of individual testing, a lower security level can be applied without compromising reliability. This requires detailed knowledge and experience and specific rules.

By ensuring that only one vehicle is on the bridge at a time, the uncertainty of the number of vehicles can be ignored. If we ensure that the vehicle is moving slowly, then the speed-dependent uncertainty can be ignored. Such measures can be found in military bridge load rating rules [6]. By applying them, higher military loads can be allowed on bridges [7].

If we know that the suspension of the vehicle in motion is particularly favourable, this also gives us the opportunity to reduce the safety level without compromising reliability [8, 9].

An expert bridge engineer can take into account additional parameters of the bridge under consideration based on knowledge and experience. The expert analysis may result in a reduction of the safety margin (e.g. very high quality, homogeneous concrete structure with detailed construction inspection, instrumented testing), but may also result in an increase of the safety margin (e.g. design and construction defects). The expert's decision may also be supported by bridge testing experience and previous inspection of similar heavy transports.

These decisions are subjective, but you must always guarantee safety. For example, the analysis may result in a reduction of the safety factor for the payload from 1.35 to 1.10 [10]. The same values are used [2] for military loads during normal crossing.

Similar results can be obtained by probabilistic analysis of safety (with consequence class and reliability index) [11], but it is important to know exactly which risk events these calculations are based on, because probabilistic methods only partially take into account the properties of a single bridge.

We can either establish general rules for military load rating [12] or consider each case individually. In the first case a larger safety margin is used, in the second case a smaller one is sufficient. The test and test load presented in the next chapter is based on an individual test. This is the reason why a vehicle with a significantly higher load capacity than the civilian bridge was able to drive on the bridge.

3 BRIDGE TEST DEMONSTRATED BY MILITARY TEST LOAD

3.1 Method for selecting the bridge

The purpose of our study was to inspect a major existing road bridge for military traffic needs. The bridge under study was selected according to the following criteria.

A Leopard armoured personnel carrier was required for the study. In Hungary, Leopard2 A7 main battle tanks are located in the city of Tata (Hungarian Defence Forces 1st Armoured Brigade „Klapka György“), so it was important that the bridge was not too far from the city of Tata.

In terms of load verification, we were looking for a bridge with a medium load capacity (max 40 tonnes). Thus, the military load tested could be significantly higher than the load capacity of the bridge.

For the test we looked for a structure with a large spaning. A large bridge can accommodate and position the payload in multiple positions and the deformation of the bridge can be measured more easily. The selected bridge had a span of 36 m (see Figure 2).

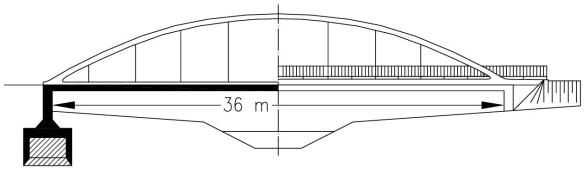

Fig. 2 Longitudinal section and side view of the selected bridge at Kecskéd
Source: author.

Furthermore, when choosing the bridge, we also took into account the environment: the civil traffic volume, what is under the bridge, how to organise the test load, how to install the measurement equipment.

The selected bridge, which meets the criteria, is located on the border of the village of Kecséd. The bridge is 18 km away from the city of Tata.

3.2 Data of the bridge under study

The road bridge over the Átal river (road sign 8155, 0+118 km) was built in 1965. It was designed by Dr. Pál Lipták. The bridge is a single-span, reinforced concrete arch bridge with lower deck. The deck is a post-tensioned reinforced concrete slab. An interesting feature of the bridge is that there is no cross stiffening (over the carriageway) between the two arches (Fig. 3).

The carriageway is 7.00 m wide. The bridge does not have bearings (Fig. 2). Its appearance is elegant and clean.

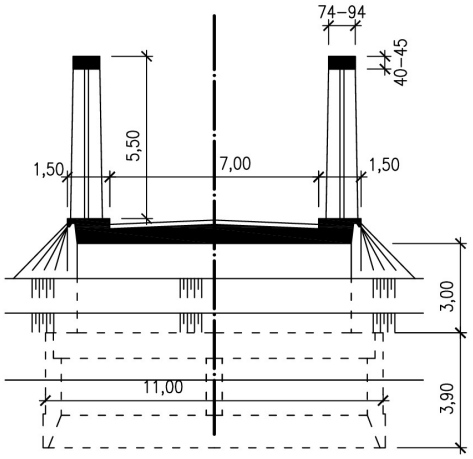

Fig. 3 Cross section of the bridge under study
Source: author.

The bridge designs are in accordance with the 1956 Hungarian Bridge Code, with a B-sign payload. The live load was one 30-ton truck (Fig. 4) with a simultaneous surface distributed load of 300 kg/m^2.

The concrete material quality of the bridge's main girder was B400, which corresponds to concrete quality C25/30. The material quality of the steel suspension rods was A.36.24, which corresponds to steel grade S235. The ultimate tensile strength of the high-strength wires used for post-tensioning was 990 N/mm^2.

The bridge was completely renovated in 2011. At that time, new waterproofing and asphalt pavement were installed on the bridge.

The last independent expert inspection of the bridge was in 2021. (Such an instrumental and detailed inspection is required every 10 years in Hungary.) The inspection found no significant defects on the bridge.

3.3 Static analysis

The bridge is designed for a 30 tonne truck and a simultaneous distributed load of 300 kg/m^2. A schematic of one vehicle considered in the static calculation is shown in Fig. 4.

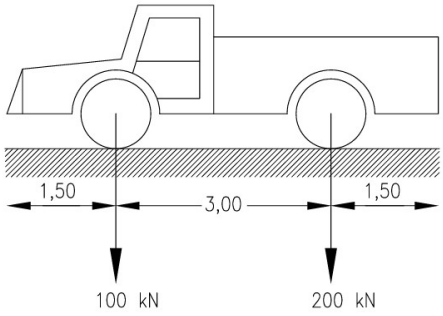

Fig. 4 Live load in the design code 1956
Source: author.

According to the factors in the 1956 Hungarian Bridge Design Code, the civil load capacity of the bridge is 40 tonnes. This means that the bridge can be used by any normal vehicle up to 40 tonnes. Vehicles heavier than this, such as Leopard tanks (63 t) and heavy machinery transporters (105 t), are not allowed on the bridge.

Two independent static calculations were carried out. The first calculation was based on the original structural analysis of the bridge (1965), replacing the payload by the military load.

The second calculation was performed using an AXIS VM finite element model calculation on a computer with the same level of detail as the design of the new bridges (Fig. 5). No material tests have been performed.

Both calculations were compared with the test load carried out when the bridge was completed in 1966. At that time, three trucks were used to load the bridge in nine load positions. The total load applied was 39.3 t.

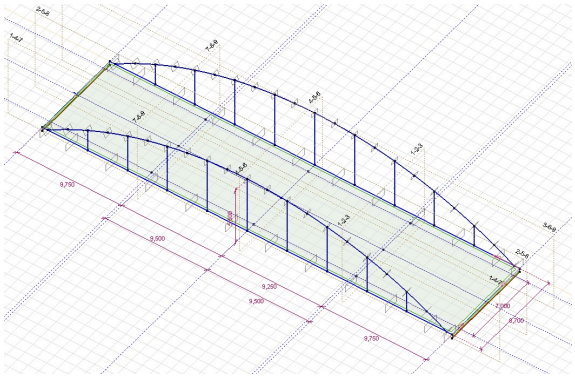

Fig. 5 The finite element model view
Source: author.

Using the safety factors in today's hungarian bridge design standards [13], the detailed calculation showed a 9 % exceeding. This was considered acceptable, given the stringent conditions associated with the test load, the most important of which were: detailed bridge inspection before and after, expert on-site supervision, measurement of bridge deflection under gradual loading, preliminary weighing of the test vehicles.

3.4 Proff-test load

After detailed preparation, the test load was on 27 November 2024. The test load plan was approved by the hungarian transport authority and the measurements were agreed by the Hungarian National Roads Administration and the Hungarian Defence Forces.

Before the test load, the Hungarian National Roads Administration checked the weight of the empty and loaded heavy equipment trailers by mobile weighing. The results of the weighing were: empty heavy equipment transporter 42 t, Leopard2 A7 63 t (Fig. 6), heavy equipment transporter with Leopard2 A7 105 t.

Fig. 6 Leopard MBT on the bridge
Source: Photographed by Benedek Kapin.

During the test load, inductive displacement sensors were used to measure the vertical deflection of the bridge at 9 points, the same locations as the 1966 test load. With the computer-aided measurement technique, dynamic measurements could be made in addition to static measurements.

The test load was scheduled for the night period to minimise possible disturbance to civilian traffic.

The measurement system was first tested with a 22 t agricultural tractor, using static and dynamic measurements.

The total test load program included 37 load positions (15 static, 22 dynamic). The sequence of load positions caused a progressive load on the bridge, so that the last load position had the highest load of 105 t. Between the loads, we could immediately check the deformation of the bridge by comparing the measured and calculated values. These checks confirmed the accuracy of the calculations, so the test load could be continued as planned up to the maximum design load.

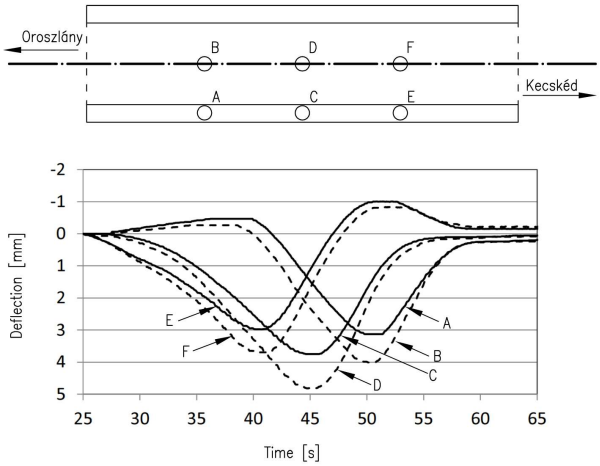

Fig. 7 Location of the measuring points
and the deflections under the 105 t military load
Source: author.

The maximum deflection measured at the centre of the bridge opening at the line of the main arch under the maximum load was 3.75 mm with dynamic measurement (5 km/h uniform speed; direction: from Kecskéd to Oroszlány). The calculated deflection with static load was 6.65 mm. The percentage of the measured value was lower than the usual experience with test loads (56 %). The lower deflection confirms the more load carrying capacity of the bridge. The Fig. 7 shows the largest deflection at the middle point of the bridge: 4.81 mm. Here, the deflection of the main girders is added to the excess deflection of the cross-section (1.06 mm).

The modulus of elasticity and strength of the concrete were calculated based on the original plans. It can be expected that the concrete properties of the constructed bridge structure are more favorable.

Conservatively, the original load capacity is recorded in the civil registry as 40 tons. This calculation took into account a 30-ton vehicle and distributed load. The total distributed load on the 7 m wide carriageway across the 36 m long opening is 75.6 tons. This means that the total vehicle load

is 105.6 tons. This is the reason why the given bridge can carry a military vehicle weighing 105 t.

4 SUMMARY

In this study, we have shown why different parameters can be used in military and civilian load capacity assessment and how higher military load capacities can be justified.

We have demonstrated by calculations that a bridge with a span of 36 m and a nominal load capacity of 40 tons can be safely used under appropriate conditions with a military load of 105 tons (Fig. 8).

The correctness of the calculation was demonstrated by a test load. The test load proved the validity of the calculation and also showed the additional capacity reserves of the bridge.

Similar test loads can provide a number of additional experiences and results for the evaluation of military bridge load capacity. A detailed processing of the test load and analysis of the nearly one million measured deflection values recorded is expected to provide further scientific results. After a detailed analysis of the test load, it is worthwhile to continue the initiated experiment, e.g. by investigating the combined effect of several military vehicles or the behaviour of a complex bridge structure under military loading.

Fig. 8 Full military load on the bridge (105 t)
Source: Photographed by Dominik Mák.

Acknowledgments

I would like to thank the Hungarian Defence Forces 1st Armoured Brigade „Klapka György“ (military load vehicles, military insurance), the Hungarian Public Roads (standard weighing of load vehicles), FAÉK Méréstechnika Ltd. (measuring technology), Cardium Ltd. (auxiliary structures) and Tibor Rák (agricultural load vehicle) for their selfless support and help in the problem-free execution of the test load.

References

[1] HAJÓS, B. Movement of overload military and civil vehicles on road bridges. In *Katonai Logisztika 2024/1-2*. Budapest pp. 230-247. Available at: https://doi.org/10.30583/2024-1-2-230

[2] HLINKA, R., FARBAK, M. and ODROBIŇÁK, J. The use of up-to date analyses for the temporary bridges application in the present. In *Civil and Environmental Engineering,* 2024, Vol. 20, Issue 1. 491-507. Available at: https://doi.org/10.2478/cee-2024-0038

[3] VIČAN, J., ODROBIŇÁK, J. and GOCÁL, J. Determination of road bridge load carrying capacity. In *Civil and Environmental Engineering,* 2021, Vol. 17, Issue 1. 491-507. Available at: https://doi.org/10.2478/cee-2021-0030

[4] VIČAN, J., GOCÁL, J., ODROBIŇÁK, J. and KOTEŠ, P. Existing steel railway bridges evaluation. In *Civil and Environmental Engineering,* 2016, Vol. 12, Issue 2. 103-110. Available at: https://doi.org/10.1515/cee-2016-0014

[5] VAVRUŠ, M., BUJŇÁK, J. and KOTEŠ, P. Experimental verification of real behaviour of bridge structure using proof-load tests. In *Pollack Periodica,* 2019, Vol. 14, No 1. 75-84. Available at: https://doi.org/10.1556/606.2019.14.1.8

[6] AEP-3.12.1.5 NATO Standard Military Load Classification of bridges, ferries, rafts and vehicles. Edition B Version 1, November 2024.

[7] HAJÓS, B. Some additional aspects for the regulation of the military load classification of existing road bridges (STANAG 2021). In *Science & Military,* 2024, Vol. 19, Issue 1. Liptovský Mikuláš: Armed Forces Academy of General M. R. Štefánik. pp. 14-19. Available at: https://doi.org/10.52651/sam.a.2024.2.14-19

[8] HAJÓS B. A közúti hidak dinamikus tényezőjének csökkentési lehetőségei túlsúlyos civil járművek és nehéz katonai szállítások esetén. In *Útügyi lapok,* 2024 (19). Available at: https://doi.org/10.36246/UL.2024.1.03

[9] HAJÓS, B. Safety and dynamic factors for determining the military load capacity of the road bridges. In *Hadtudomány*, 2024, Issue 2. Budapest. pp. 101-113. Available at: https://doi.org/10.52651/sam.a.2024.2.14-19

[10] LENNER, R. *Safety Concept and Partial Factors for Military Assessment of Existing Concrete Bridges.* PhD Dissertation, Universität der Budeswehr Müchen, Fakultät für Bauingenieurwesen und Umwelt-wissenschaften, 2014.

[11] LENNER, R. Partial factors for loads due to special vehicles on road bridges. In *Engineering Structures,* 2016, Issue 106, pp. 137-146. Available at:

https://doi.org/10.1016/j.engstruct.2015.10.024

[12] HAJÓS, B. and GOSZTOLA, D. Proposals for the Military Load Capacity Assessment of Existing Road Bridges. In *11th International Conference on Bridges in the Danube Basin (ICBDB2024).* Munich: Technical University of Munich, 20th to 21st November 2024. pp. 307-317.

[13] e-UT 07.01.12:2011 Erőtani számítás közúti hidak tervezése (KHT) 2. Útügyi Műszaki Előírás. (Static calculations for road bridge design. Hungarian Road Engineering Technical Specifications). Available at: https://ume.kozut.hu/dokumentum/745

Dipl. Eng. Bence HAJÓS
Ludovica University of Public Service
Ph.D. student, Doctoral School
of Military Engineering
Nap utca 6.
4024 Debrecen
Hungary
E-mail: elsolanchid@elsolanchid.hu

Bence HAJÓS received a M.Sc. (Eng.) from the Budapest University of Technology and Economics (BME) in Hungary in 2001, in bridge engineering.

Until 2014, he worked in the operation and maintenance of road and rail bridges. He is currently a private engineer, bridge inspection expert. His main research interests are bridge load capacity assessment, existing bridges, overload transports and bridge history.

His research interests include the assessment of the military load capacity of existing road bridges in preparation for PhD degree at the Ludovica University of Public Service (Budapest).

DOI: https://doi.org/10.52651/sam.a.2025.1.11-15

OPERATIONAL USE OF MULTISPECTRAL METHODS AGAINST UAS EFFECTS

Robert ROZGONYI

Abstract: Unmanned Aerial Systems (UAS) have become a pivotal component in modern warfare and civil applications, offering unmatched flexibility, mobility, and operational capabilities. With the integration of artificial intelligence and lightweight materials often enabled by 3D printing UAS are increasingly difficult to detect and neutralize. This article focuses on methods for the effective localization and identification of UAS, particularly through the use of multispectral cameras that operate across different bands of the electromagnetic spectrum. However, it is evident that relying solely on optical systems, even advanced ones, is insufficient for accurate detection, especially in complex terrain or at extended ranges. To address this challenge, a multi-sensor approach is proposed, integrating optical, thermal, and radar data for enhanced situational awareness. Key requirements for anti-UAS systems are outlined, including high sensitivity, real-time data sharing, distinction between UAS and natural objects, and the ability to counter both wirelessly and optically controlled drones. The study also discusses the emerging threat posed by optically tethered drones, which bypass standard jamming techniques. The broader implications of UAS technology are considered, from battlefield dominance to humanitarian uses such as search and rescue and infrastructure monitoring. This research underscores the urgency for adaptive, multi-modal counter-UAS systems as the technology continues to evolve rapidly.

Keywords: multispectral methods, UAS effects, localization.

1 INTRODUCTIONS

Currently, UAS is one of the most difficult to localize enemy combat systems. To accurately localize them, several sensors operating in different spectra are needed to determine their position with the highest possible precision. Protecting our units leads us to consider how to defend against such devices, how to affect them, or even destroy them. In the near future multiple UAS are expected on the battlefield, so we need to localize as many of them as possible. Due to their wide range of uses the localization of UAS must be as fast as possible. Nowadays, UAS represent one of the most dangerous means of warfare due to their variations, and their usage is uncountable. With the help of artificial intelligence, they represent one of the most sophisticated tools of the future. To localize UAS we will use a multispectral camera that operates across multiple spectra, allowing us to detect even relatively small and distant objects at greater ranges. There are several manufacturers attempting to design their UAS with the lightest materials making them faster. With the advent of 3D printers, this process is accelerating even more as these UAS are made with fewer metal parts, or their bodies are covered, making them increasingly difficult to detect. Manufacturers of such UAS are working on their concealment and detection.

UAS are used for example in detailed terrain surveys, where they can operate in harsh conditions day and night. They can transport necessary materials even explosive devices, and are capable of creating 3D models by mapping the environment. Another feature of UAS is that they can record in real time. They can be controlled and powered by an optical cable over a certain distance. They are capable of carrying explosive payloads, where the target has no opportunity to escape, if once locked onto a target, they can glide towards it. The use of UAS as light carriers or speakers these possibilities provide UAS with countless additional uses. Some UAS offer the option to control them with two transmitters, one for the pilot and the other for the cameraman. This capability suggests that in the near future, there may be an opportunity to control UAS by multiple operators simultaneously. [1]

Fig. 1 FPV UAS with explosive device
Source: author.

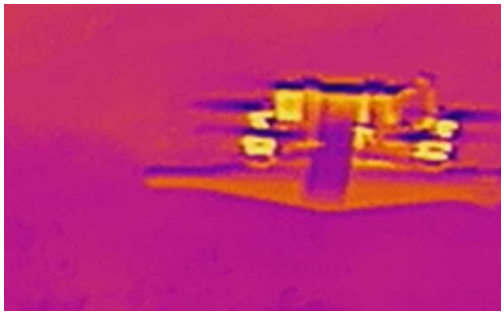

Fig. 2 FPV UAS with explosive device in thermal cameras distance 50 meters
Source: author.

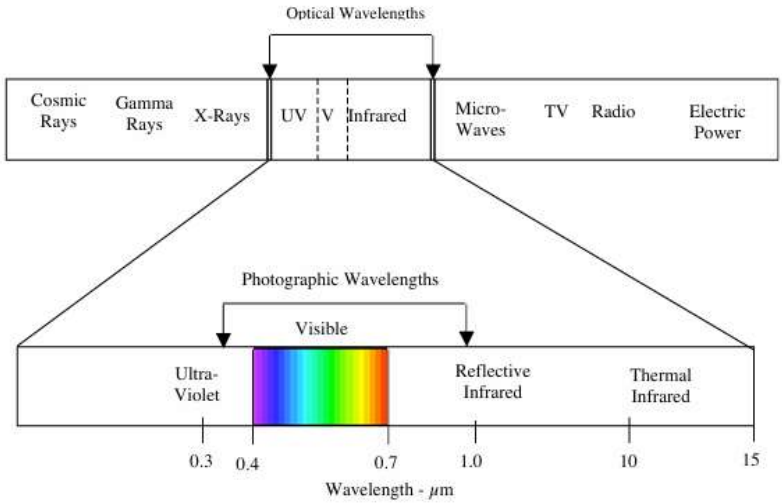

Fig. 3 The Elektromagnetic Spectrum
Source: [2].

„Optical telescopes consist of optical elements such as lenses, mirrors, and optical prisms. Optoelectronic devices also include other systems that assist in observing objects, displaying reticle patterns, and adding various information to the optical output."

Optical devices can be divided into several areas of electromagnetic radiation.

Tab. 1 Division of electromagnetic radiation

Visible light (VIS)	0,38÷0,78 μm
Near infrared region (NIR)	0,78÷2 μm
Mid infrared region (MIR)	3÷5 μm
Far infrared region (LWIR)	8÷14 μm

Source: [3].

In the infrared radiation range between wavelengths of 5-8 μm, there is a high degree of radiation absorption. The absorption of radiation is caused by gas molecules (O_2, O_3, CO_2, H_2O, NO_2, and so on). It can be assumed that this gap will beutilized by UAS manufacturers. To prevent such an occurrence, the solution is the combination of their detection in multiple spectra.

I will present several requirements for manufacturers of anti UAS devices that need to be defined for the device to successfully locate UAS. The sensitivity of the device should be such that it can distinguish UAS of even the smallest sizes (few centimeters) and differentiate it from flocks of birds. Another distinction will be whether it is a single UAS or several UAS, or whether it is our own UAS or an enemy one. It is necessary to gather information on whether the UAS is controlled by electromagnetic waves or optical fibers, as we can influence it by other means. Advantageous information would also include the precise location of the UAS and its operators. If the device could detect the UAS's MAC address, it would be easier to influence it if we know its operational frequencies. Detection should be at a range where even a UAS that can lock onto its target would not have the opportunity to reach its destination.

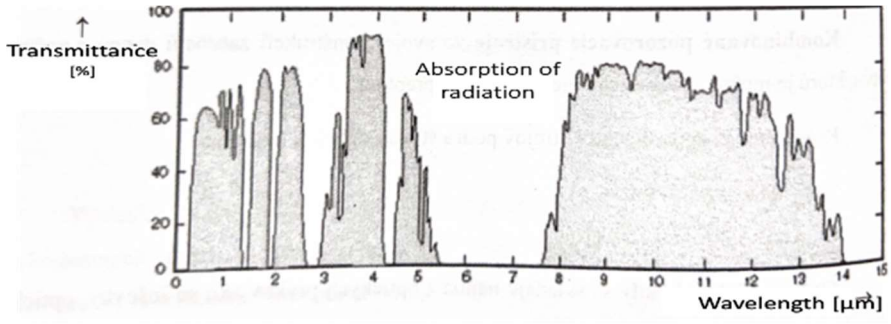

Fig. 4 Radiation transmittance through the atmosphere
Source: [3].

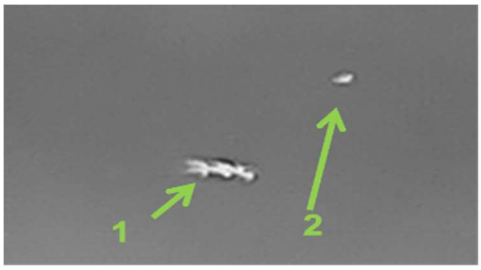

Fig. 5 The object 1 is UAS, object 2 is eagle distance 300 meters
Source: author.

The ideal solution would be the creation of a cover, ensuring that each of our units (vehicles) includes a device for localization, and each would share information with the others, thereby creating a kind of shield to secure the most reliable coverage of our positions.

The proposed requirement for manufacturers is to ensure data sharing about the detected device and secure coverage over our units. Therefore, I propose creating an imaginary shield to ensure the coverage of adjacent vehicles.

Fig. 6 UAS in visible
view distance 200 meters
Source: author.

Fig. 7 UAS in infra camera
view distance 100 meters
Source: author.

Fig. 8 UAS in thermal camera
view distance 50 meters
Source: author.

I assume that a combination of sensors is necessary for the identification and localization of UAS including multispectral cameras, radars, etc. After localization we need to act on them using one of the available methods such as physical destruction, possible neutralization, taking control of the device, or destruction.

In Fig. 6, the UAS is captured using a multispectral camera in daytime mode. The image clearly shows that the UAS, which is hovering silently in the air, is nearly impossible to detect when positioned against a forested background. In Fig. 7, the UAS is shown using a multispectral camera in infrared mode. The image clearly demonstrates that the UAS, while hovering in the air, is very difficult to recognize when positioned against a forested background. In Figs. 2 and 8, the UAS is shown using a multispectral camera in thermal mode.

The image shows a UAS hovering in the air, which is very difficult to identify when positioned against a forested background. Thermal radiation is only visible on certain parts of the UAS. The arrival of UAS controlled via optical cables represents another threat to our units. This is a phenomenon that adds a new dimension to the fight against UAS devices. This type of UAS controlled via optical cables is very difficult to counter with standard jammers, and another advantage is their continuous power supply via the cable. Therefore, they need to be destroyed in another way.

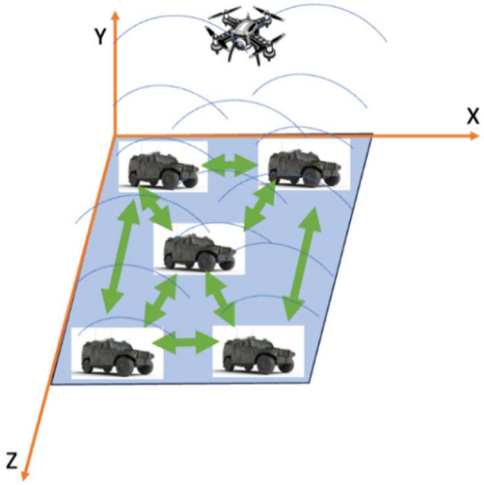

Fig. 9 Cover abow vehicles
Source: author.

To understand its operation and focus on the shortcomings of UAS, it is necessary to start with UAS manufacturers. Today we know hundreds of UAS manufacturers and thousands of distributors. One of the basic divisions is whether the UAS is for the mass market, professional use, or military purposes. For the operator to be effective, they must take into account. First changing altitudes by following the terrain and changing speed. In some cases the speed of UAS exceeds 100 km/h. Factors that affect flight duration include battery capacity, weather conditions, and of course the weight of the UAS itself. The weight is influenced

by the equipment such as additional batteries and various sensors. One of the most difficult factors to influence is the weather, including wind. Therefore, the UAS must constantly stabilize and adjust to stay on course. Another factor is frost, as the air temperature significantly weakens battery capacity. The combination of cold and humidity negatively affects flight performance. Lastly humidity doesn't necessarily mean that some UAS are not adapted to fly in the rain, but humidity adversely affects the rotary elements. The worst element is the combination of cold and humidity, as ice can form on the rotating blades. Ideal weather conditions are around 20°C with no wind. Weight is also negatively influenced by the choice of construction material, which is crucial for UAS depending on where it will be used. Commercial UAS are made of plastic, and the availability of spare parts is adequately secured. However, some materials such as carbon fibers, offer excellent properties in terms of weight and quality. Additionally, we may encounter materials like duralumin or fiberglass.

The selection of a camera for UAS presents another range of possible uses, one of which is a thermal camera, which has numerous applications. Among the most interesting for us is the multispectral camera, which in addition to the three basic RGB channels has additional channels. They most often have four channels: blue, green, red, and near infrared. [4]

The main advantages of UAS compared to manned machines are their lower operating costs enormous flexibility in space, and the ability to be used indoors. They also have low noise during operation and can land in difficult to reach places. The biggest advantage is their quick deployment capability, and not to be overlooked is their price. Development in the UAS field is progressing at an incredible speed, and this has led to advancements in high-end cameras, photo devices, and sensors. Their weight is rapidly decreasing, but the quality of the recordings is much better. The advantages of military UAS are their operational time, as they can fly with combustion engines, however this affects the size and weight of the device. The disadvantage is that UAS do not have transponders like manned aircraft, making them difficult to identify and track. This can pose a risk to air traffic safety, especially when manned aircraft are operating in the same airspace. Without a transponder, air traffic controllers and other pilots are not aware of the UAS presence, which can lead to dangerous situations or collisions. [5]

Some UAS are still in development, but the rapid evolution of these devices has led to incredible progress. They are capable of flying at hypersonic speeds, allowing them to destroy strategic targets. Furthermore, they can support air operations as they act as auxiliary units. These UAS accompany the main combat vehicle controlled by a pilot, with the pilot assigning them various tasks to destroy different targets. The greatest advancement is a UAS that can autonomously decide and carry out tasks with the assistance of an operator. Another possible scenario is that the operator will only monitor the situation, and the UAS will make its own decisions. [6]

2 SUMMARY

The issue of UAS localization is currently something that must be given as much attention as possible as they represent a revolutionary breakthrough in battlefield combat. Their development is progressing very quickly, which means countermeasures against them are also necessary. Therefore, I have presented several requirements for manufacturers regarding UAS localization and later optimal methods of counteracting them. After evaluating all the factors influencing the detection of UAS, and as demonstrated in the previous research images, it is evident that a standalone multispectral camera even with a wide field of view is not capable of accurately detecting UAS, especially at longer distances and difficult terrain.

This finding highlights a critical limitation in relying solely on optical systems for effective UAS detection. As a result, future research will focus on the integration of multiple sensors to improve detection accuracy and reliability. By combining data from different sensing technologies, it may be possible to overcome the individual limitations of each system and achieve a more robust and scalable solution for UAS monitoring.

The use of UAS brings a kind of freedom to combat, and their application in all sectors represents their use in almost all areas.

UAS are no longer used only on the battlefield today, but also in other sectors where there is a need to save human lives. There is a high likelihood that in the future, these devices will be used for example in fire protection, in healthcare for the transportation of the injured from difficult-to-reach terrain, and also for detecting damage to various infrastructures.

References

[1] KOCOUREK, J. J. *Drony: Praktická příručka pro majitele dronů DJI.* Vol. 2. Praha: 2019. pp. 73-152. ISBN 978-80-7346-228-4.

[2] LANDGREBE, A. D. *Signal theory methods in multispectral remote sensing.* New Jersey: 2003. pp. 14. ISBN 0-471-42028-X. Available at: https://doi.org/10.1002/0471723800

[3] BRIDIK, L. *Optické a optoelektronické prístroje.* Liptovský Mikuláš: Akadémia

ozbrojených síl generála M. R. Štefánika, 2018. pp.72-74. ISBN 978-80-8040-573-1.

[4] KARAS, J. *222 tipů a triků pro drony*. Brno: Computer Press, 2017. pp. 25-147.ISBN 978-80-251-4874-7.

[5] KARAS, J. a TICHÝ, T. *Drony.* Praha: Computer Press, 2016. pp. 33-195. ISBN 978-80-251-4680-4.

[6] STILWEL, A. *Vojenské drony: nepilotované letouny*. Prešov: Universum, 2024. pp. 77-141. ISBN 978-80-242-655-5.

2nd Lt. Eng. Robert **ROZGONYI**
Ph.D. student, Department of Mechanical Engineering
Armed Forces Academy of General M. R. Štefánik
Demänová 393
031 01 Liptovský Mikuláš
Slovak Republic
E-mail: robert.rozgonyi@aos.sk

Robert ROZGONYI was born in 1982 in Kraľovský Chlmec. He is currently studying external PhD. at Department of Mechanical Engineering in Armed Forces Academy of General M. R. Štefánik. His research area mainly includes multispectral methods in military technologies.

DOI: https://doi.org/10.52651/sam.a.2025.1.16-29

TRIBOTECHNICAL DIAGNOSTICS – ANALYSIS OF ENGINE OIL DEGRADATION VIA OIL PROPERTIES OF SAE 10W-30 IN TATRA PHOENIX DURING 9 MONTHS OF USE

Adam FULEK, Vladimír KADLUB, Miroslav MARKO

Abstract: This article discusses selected degradation elements in the context of tribodiagnostic measurement. Four engine oil (EO) measurements were made to monitor changes in selected properties during 4,546 km of operation. EO samples were taken from the Tatra 815 Phoenix at three-monthly intervals. All samples were measured in the tribodiagnostic laboratory of the Armed Forces Academy, Department of Mechanical Engineering, on SpectroVisc Q-3050, Spectro Q1000 Fluid Scan, SpectroCube, FeroCheck and an electron microscope to perform photo-documentation of the separation membrane and separation filter results. The paper presents the measurements on the SpectroCube, FeroCheck and the electron microscope in more detail.

Keywords: engine oil, kinematic viscosity, Ferrocheck, TBN, TAN, glycols, water, soot, nitration, oxidation and individual elements of the periodic table.

1 INTRODUCTION

Engine oils and their properties are very important parameters when monitoring the technical condition of the engine. Every single EO must meet certain requirements and properties prescribed by the manufacturer at a predefined interval in the process of operation. For each type of internal combustion engine a certain type of EO is prescribed, with a given viscosity and performance specification. During vehicle operation, EO degradation occurs depending on the load and the number of operating units of the vehicle.

Fig. 1 Vehicle Tatra Phoenix 815
Source: author.

2 USAGE ENGINE OIL

Engine oil DAF engine oil psql 2.1E, SAE 10W-30, fully synthetic, suitable for Euro 4,5,6 engines. It is designed for new low emission engines. ACEA E7, E9 specification; API specification CI-4+, CJ-4. [1]

3 VEHICLE TATRA 815 PHOENIX

The Tatra 815 Phoenix is of a flatbed construction and is designed for transporting materials and people on paved roads and off-road terrain. Its power unit is a DAAF engine with the PACCAR MX-13 designation. The MX-13 engine is a 12.9-litre diesel engine with 355 kW at 1,600 rpm and 2,350 Nm of torque. Exhaust gas recirculation via EGR is also incorporated in the engine design. [7]

Fig. 2 Engine PACCAR MX-13
Source: [7].

Tab. 1 Parameters of engine oil from manufacturer

Feature	Unit	Value
Density at 15 °C	[kg/l]	0,87
Density at -25 °C	[mPa.s]	5830
Density at 40 °C	[cSt]	80,2
Density at 100 °C	[cSt]	11,9
Viscous index	-	142
Ignition point	[°C]	224
Freezing point	[°C]	-42
TBN	[%]	9,8

Source: author.

4 KINEMATIC VISCOSITY ANALYSIS

Kinematic viscosity (KV) is a carrier parameter in EO evaluation, it addresses the issue of EO fluidity, which is measured by the flow rate through the calibration unit (mm2) per time (t) reported in units of mm2/s (cSt). The range of applicability of the EO according to our criteria is within ± 20 % of the reference sample values. EO manufacturers report the KV at two temperatures, namely 40 ˚C and 100 ˚C. The measurements were performed on a SpectroVisc Q-3050 measuring instrument. The graph of the KV at 40 and 100 ˚C shows the trend of the KV and the arrows shown below the graphical representation tell the trend of the KV during the course of the vehicle operation. All measured KV values met the EO serviceability condition within ± 20 %. [6,5,11]

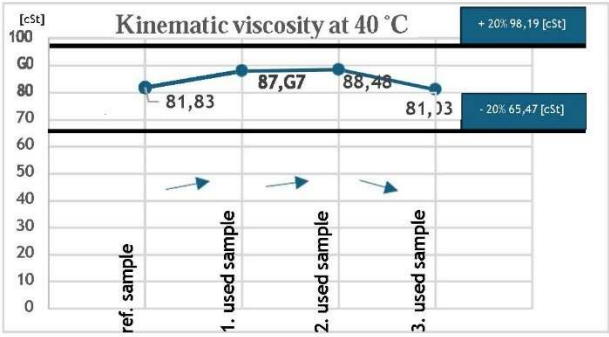

Fig. 3 Graph of kinematic viscosity 40 ˚C
Source: author.

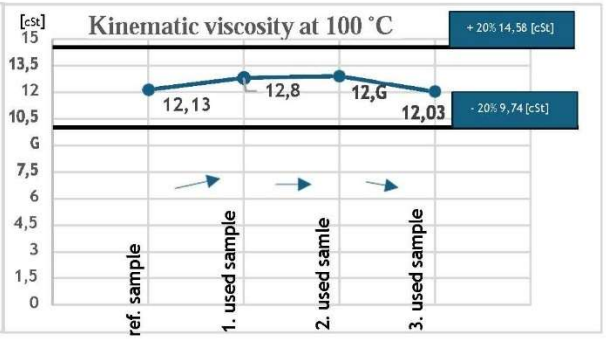

Fig. 4 Graph of kinematic viscosity 100 ˚C
Source: author.

Tab. 2 Summary overview of KV

Feature	Unit	Referential sample	Sample No.1	Sample No.2	Sample No.3
Date of collection	[d.m.y]	23.02.2024	21.02.2024	22.05.2024	04.09.2024
Date of measurement	[d.m.y]	23.02.2024	23.02.2024	12.07.2024	06.09.2024
Millage of EO	[km]	0 (EO change)	1 821	1 986	4 546
Millage of vehicle	[km]	13 080	14 901	15 066	17 626
Kinematic viscosity at 40 ˚C	[cSt]	+20% [%] 98,19 [cSt] 81,83 -20% [%] 65,47 [cSt]	87,97 +7,49 [%] // +6,14 [cSt]	88,48 +8,13 [%] // +6,65 [cSt]	81,03 -0,98 [%] // -0,8 [cSt]
Kinematic viscosity at 100 ˚C	[cSt]	+20% [%] 14,58 [cSt] 12,3 -20% [%] 9,74 [cSt]	12,8 +5,52 [%] // +0,67 [cSt]	12,9 +6,35 [%] // +0,77[cSt]	12,03 -0,82 [%] // -0,3[cSt]

Source: author.

The table shows the progression of the individual values in the selected parameters. For the reference sample KV (40 and 100 ˚C) the range of applicability is given. For the oils used (sample 1, 2, 3), the calculation of the tendency of increase or decrease of KV in [%] and [cSt] is made. In terms of KV, the EO is in good condition (specified range ± 20 %) and is usable in service without limitations. [6,5,11]

4.1 Linking Diagnostic Methods in the Evaluation of MO

The influence of diagnostic methods on the determination of qualitative parameters of MO is considerable. With the addition of MO tribodiagnostics characteristics, it is appropriate to use vibrodiagnostics to characterize the transmission of unwanted frequencies from the engine to the crew. For this purpose, modern and accurate diagnostic instruments are needed that can specify the vibrations encountered and the possibility of their modification in operation, since a certain frequency modulation has a significant impact on the ergonomics and the health of the crew. One method of reducing the transmission of frequency modulation is to change the viscous characteristic of the MO. The use of general knowledge of the use of diagnostics and tribodiagnostics allows us to improve the characteristics of the vehicles used and, in particular, to detect undesirable effects in newly introduced technology. [13,14]

5 MONITORED PROPERTIES OF EO

As an additional measurement to determine the status of the EO, a measurement was performed

on the Spectro Q100 Fluid Scan to detect the change in the status of the following EO parameters [12]:

Total additivity [%] - a certain amount of additive elements are present in each EO and other lubricants. These elements guarantee and improve the properties of oils and lubricants. The value and type of these elements vary depending on the manufacturer and the type of lubricant. As the value of the total additive decreases, the properties of the EO are expected to decrease. When the total additivity drops below 30 [%], the applicability of EO with other measured properties is considered. Increased additivity between second and third sample was due to adding fresh engine oil to engine. It happened during periodic care of vehicle by driver. [8,11,5]

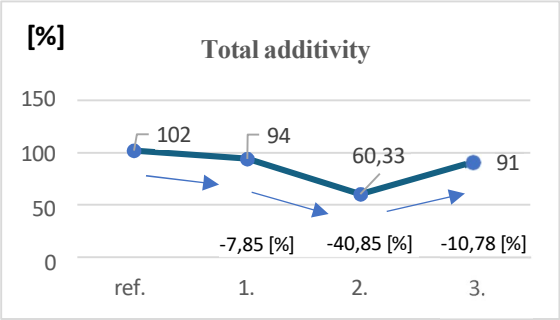

Fig. 5 Position No. 1 in table n. 3
Source: author.

Glycols [%] - in the chemical reaction of glycol compounds (Ethylene Glycol-C2H6O2, or Propylene Glycol-C3H8O2) with additives and base EO components (petroleum, semi-synthetic and synthetic). This process causes the separation of the additives from the base EO component. The presence of glycol compounds is unacceptable and causes densification of the EO. [8,11,5]

Nitration/Nitritation [abs/cm] ** - Caused by nitration products of NO2 components to organic compounds and decomposition of additives in EO. The compliant range for these elements is ± 20 % compared to the reference sample values. It is a negative parameter in EO. [8,11,5]

Oxidation [abs/cm] ** is the oxygen content absorbed by the EO during the process of operation in the engine. EO is not naturally resistant to oxidation and therefore it is necessary to use antioxidant additives. The amount of oxidation is unsatisfactory if the antioxidant content drops below 50 % of the value compared to the reference sample (This value was determined by the AOS tribodiagnostic engineer). [8,11,5]

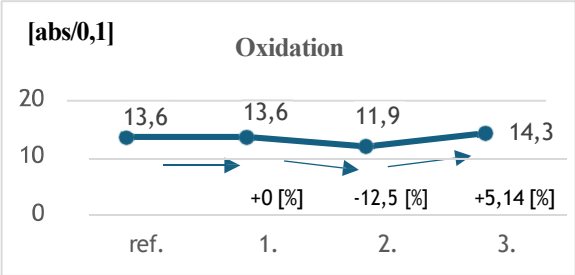

Fig. 6 Poosition No. 4 in table n. 3
Source: author.

Soot [% wt] ***** - soot is formed during combustion, especially in processes with a higher fuel content in the combustion mixture. These soot particles are trapped on the working parts of the combustion engine, where they enter the EO through the lubrication process. The unsatisfactory content of these soot particles in the EO is above 2 % (this characteristic does not mean a tribodiagnostic measurement which measures the amount of free carbon in a given sample). [8,11,5]

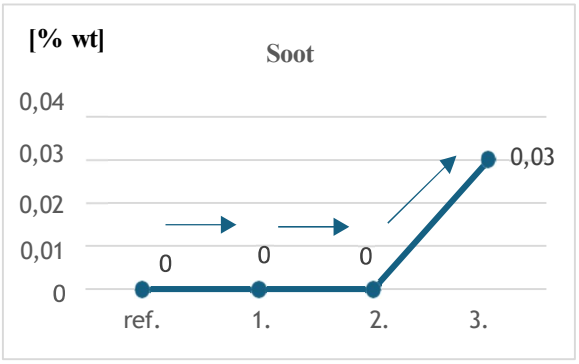

Fig. 7 Position No. 5 in table n. 3
Source: author.

Sulfation [abs/0,1] *** is the process by which so-called sulfates (salts of sulfuric acid) are formed. These processes in EO cause the separation of the additive from the base component. This decomposition is mainly caused by H2O. It is a negative parameter in EO. [8,11,5]

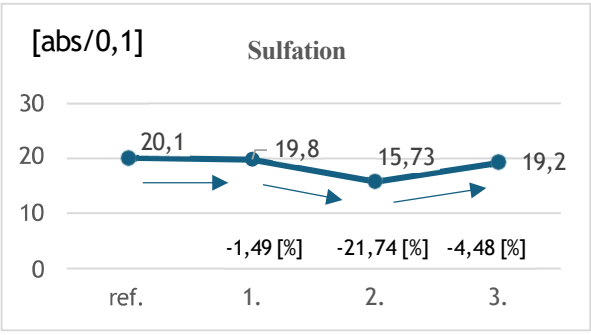

Fig. 8 Position No. 6 in table n. 3
Source: author.

TBN [mg KOH] **** - Total Basic Number (TBN), it is a EO parameter that determines the dissipation of acid sludge, indirectly expresses the service life of the oil. Too low a value in the range of -15 to -20 % expresses an unsatisfactory EO rating (This value was determined by the AOS tribodiagnostic engineer). [8,11,5]

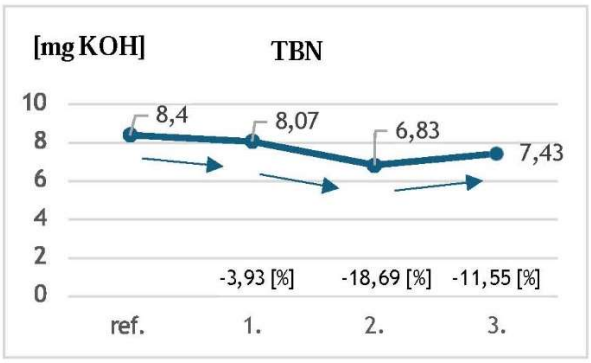

Fig. 9 Position No. 7 in table n. 3
Source: author.

Water content [ppm]* - the total water content of the EO affects the triggering of negatively influencing chemical reactions. One of them can be e.g. sulphation. These reactions cause the separation of additive elements from the base of the EO. The risk level of water in ppm units is in the range of 1000-3000 ppm (0.1-0.3 %) and at levels above 5000 ppm (0.5 %) the EO is unsatisfactory (This value was determined by the AOS tribodiagnostic engineer). [8,11,5]

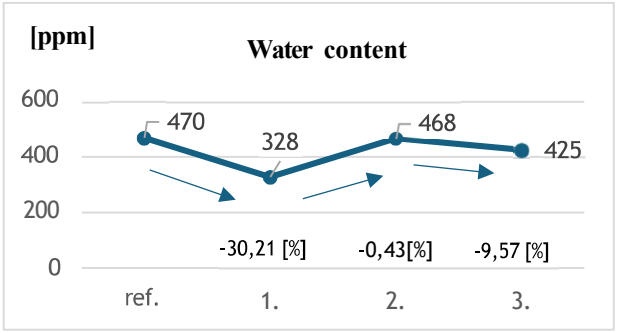

Fig. 10 Position No. 8 in table n. 3
Source: author.

Note:
*[ppm] - parts per million, 1 ppm=0.0001 %
** [abs/cm] - absorption of light by a substance per unit distance cm
***[abs/0,1] - absorption of light by a substance per unit distance of 0,1 cm
****[mg KOH] - milligrams of potassium hydroxide
*****[% wt] - unit of concentration of the mass ratio of the mixture, expressed as a percentage [4]

Tab. 3 Summary overview EO features

No.	Feature	Unit	Referential sample	Sample No.1	Sample No.2	Sample No.3
	Date of collection	[d.m.y]	23.02.2024	21.02.2024	22.05.2024	04.09.2024
	Date of measurement	[d.m.y]	23.02.2024	23.02.2024	12.07.2024	06.09.2024
	Mileage of EO	[km]	0 (EO change)	1 821	1 986	4 546
	Mileage of vehicle	[km]	13 080	14 901	15 066	17 626
1.	Total additivity	[%]	102	94 -7,85[%] // -8[cSt]	60,33 -40,85[%] // -41,67[cSt]	91 -10,78[%] // -11[cSt]
2.	Glycols	[%]	0	0	0	0
3.	Nitratation	[abs/cm]	0	0	0	0
4.	Oxidation	[abs/0,1]	13,6	13,6	11,9 -12,5[%] // -1,7[cSt]	14,3 +5,14[%] // +0,7[cSt]
5.	Soot	[% wt]	0	0	0	0,03
6.	Sulfatation	[abs/0,1]	20,1	19,8 -1,49[%] // -0,3[cSt]	15,73 -21,74[%] // -4,37[cSt]	19,2 -4,48[%] // -0,9[cSt]
7.	TBN	[mg KOH]	8,4	8,07 -3,93[%] // -0,33[cSt]	6,83 -18,69[%] // -1,57[cSt]	7,43 -11,55[%] // -0,97[cSt]
8.	Water content	[ppm]	470	328 -30,21[%] // -142[cSt]	468 -0,43[%] // -2[cSt]	425 -9,57[%] // -45[cSt]

Source: author.

6 OCCURRENCE OF METALS IN EO

This measurement was carried out on two instruments, namely the FeroCheck 2000 series, using which we detect the amount of ferroparticles in the EO (26Fe55,845; 27Co58,933; 28Ni58,693). The instrument measures the abundance based on magnetic detection.

Ferroparticle content – the occurrence in EO generally indicates the wear of the corresponding interactive surfaces of the engine. Criteria have been established for the assessment of EO (This value was determined by the AOS tribodiagnostic technician). [11,10]

- FerroCheck 2000 is set to an interface of 1,000 ppm.

- Amount <0 ppm - 30 ppm> Occurrence of ferroparticles.
- Amount <30 ppm - 70 ppm> Increased occurrence of ferroparticles.
- Amount <70 ppm - 100 ppm> Risk amount of ferroparticles.
- Amount <101 ppm and above> Intolerable amount of ferroparticles.

Tab. 4 shows the tendency of the occurrence of ferroparticles in the EO during operation. The occurrence of ferroparticles at the last measurement is 9.8 ppm. The EO is satisfactory for this test and is capable of further operation. [4,5]

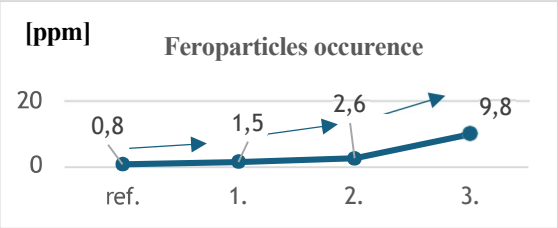

Fig. 11 Feroparticles occurrence from table No.4
Source: author.

Table 4 Measured values of metals in EO

Feature	Unit	Referential sample	Sample No.1	Sample No.2	Sample No.3
Date of collection	[d.m.y]	23.02.2024	21.02.2024	22.05.2024	04.09.2024
Date of measurement	[d.m.y]	23.02.2024	23.02.2024	12.07.2024	06.09.2024
Milage of EO	[km]	0	1 821	1 986	4 546
Milage of vehicle	[km]	13 080	14 901	15 066	17 626
Feroparticles occurence	[ppm]	0,8	1,5	2,6	9,8

Source: author.

7 AMMOUNT OF ELEMENTS

Selected elements from the periodic system that occur in EO samples are monitored and evaluated on the Spectro Cube thirobalance instrument. The instrument operates on ED-XRF technology by screening the elements in the light spectrum. As a result of the measurements, the so-called "peaks" (a graph of the pulse size and the frequency of the emitted energy) and a table with the number of elements in units of [ppm] are obtained (the content of elements is evaluated by the AOS tribodiagnostic technician). [9]

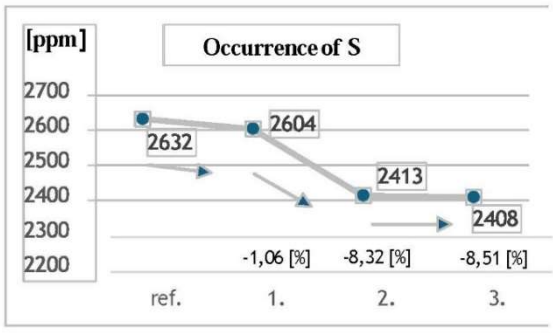

Fig. 12 Graph of sulfur occurrence
Source: author.

One of the elements monitored in the EO was sulfur, which is produced by chemical reactions and separation from the additive (fuels) during the combustion process and can cause increased corrosivity of contact surfaces. When mixed with water, strong corrosive plagues are formed. Therefore, when sulfur is detected, we determine the so-called corrosive number. A decrease due to the effect of operation has been recorded as shown in Fig. 12 [2,11].

The second element monitored was calcium, which is not directly present in the design of the Tatra Phoenix internal combustion engine. This element is used as an additive element in EO. This element improves corrosion protection, stabilization at high temperatures, wear protection and neutralizes adverse chemical reactions. The calcium occurrence in the standard ± 20 % is shown in Fig. 13. [2,11]

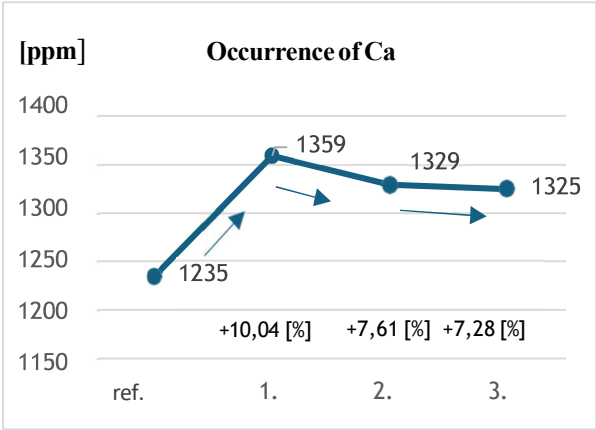

Fig. 13 Graph of calcium occurence
Source: author.

The third element studied was magnesium, which is found in EO in the form of additives that perform various functions such as acid neutralization, TBN

enhancement and wear protection. It is primarily found in detergents and neutralizing additives. Its satisfactory occurrence is shown in Fig. 14. [2,11]

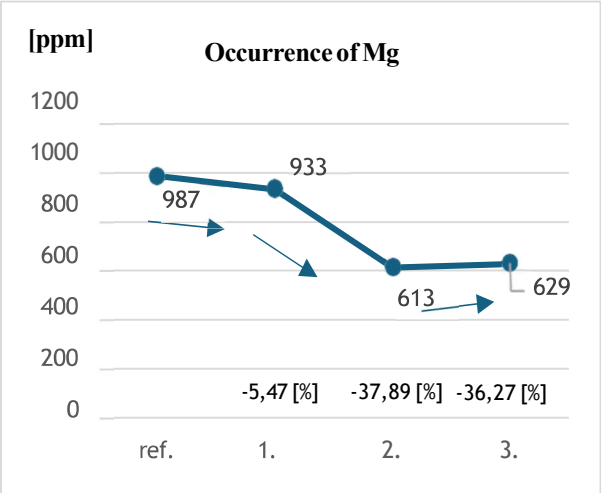

Fig. 14 Graph of magnesium occurrence
Source: author.

The fourth element monitored was phosphorus, which also occurs as many other elements in EO in the form of additives. They serve to reduce wear on the contact surfaces, retard oil oxidation and increase performance characteristics. A decrease in phosphorus has been noted. From a tribodiagnostic point of view its occurrence is satisfactory. [2,11]

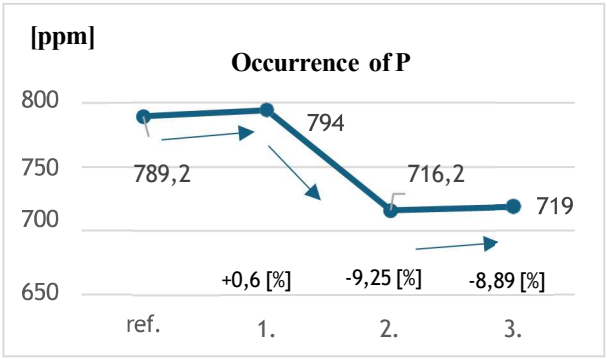

Fig. 15 Graph of phosphorus occurrence
Source: author.

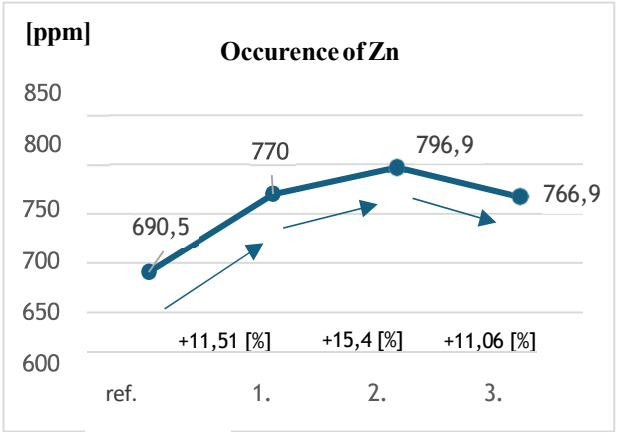

Fig. 16 Graph of zinc occurance
Source: author.

The fifth monitored element whose values we were able to measure and detect over time is zinc. Zinc is not often used as a construction material, its occurrence is again as part of the additive elements in EO. Its primary function is to form a protective coating against wear and thus increase engine life, protecting lifters, cams, piston rings and other contact surfaces. Its occurrence in measured samples is within ± 20 % of the ref. pattern. [2,11]

The sixth element monitored is chlorine, which is undesirable in EO. It causes EO contamination and results in the formation of acid sludge, reduces the effectiveness of additives and causes corrosion. Its presence in the EO may indicate poor use of additive elements with incorrect concentrations, or it may have entered the EO through cleaning elements (solvents, detergents or contaminated water) [2,11].

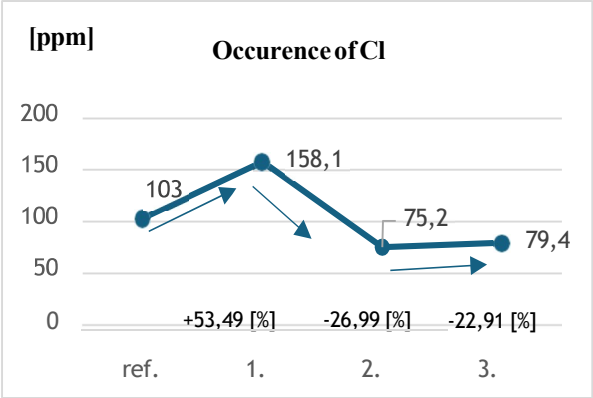

Fig. 17 Graph of chlorine occurrence
Source: author.

Silicon was the seventh element monitored. An increased abundance of silicon was measured. This increased silicon may be caused by the air filter, which may not be sufficiently capturing the impurities that enter the combustion chamber through the intake tract. There it causes excessive wear of the contact surfaces. Based on the occurrence of silicon, I decided to process a graphical visualization of its occurrence, and changes over time, along with the other pre-determined monitored elements. Due to its high abundance, its quantity is unsatisfactory. [2,11]

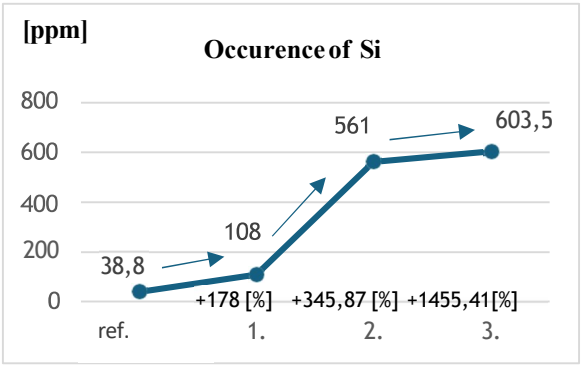

Fig. 18 Graph of silicon occurrence
Source: author.

Potassium was the last element measured or screened above 10 [ppm]. The occurrence of potassium in the EO may be due to the intrusion of coolant into the EO. Some coolants contain potassium in their composition in the form of potassium hydroxide or other salts. COD can enter the EO e.g. through a damaged cylinder head gasket, or by contamination through the EO filler holes. It is also found in some specific additives. It causes sludge formation, deposits, corrosion and thickening of EO [2,11].

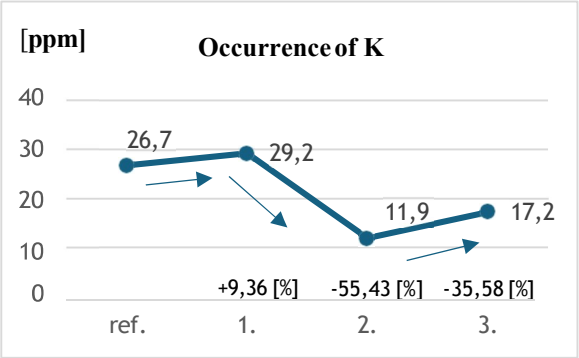

Fig. 19 Graph of potassium occurrence
Source: author.

Tab. 5 Elements occurence – SpectroCube

Feature		Referential sample	Sample No.1	Sample No.2	Sample No.3	Unit
Date of collection		23.02.2024	21.02.2024	22.05.2024	04.09.2024	[d.m.y]
Date of measurement		23.02.2024	23.02.2024	12.07.2024	06.09.2024	[d.m.y]
Milage of EO		0(EO change)	1 821	1 986	4 546	[km]
Milage of vehicle		13 080	14 901	15 066	17 626	[km]
Sign	**Element**	**Amount**				
S	Sulfur	2632	2604 -1,06[%] // -28[ppm]	2413 -8,32[%] // -219[ppm]	2408 -8,51[%] // -224[ppm]	[ppm]
Ca	Calcium	1235	1359 +10,04[%] // +124[ppm]	1329 +7,61[%] // +94[ppm]	1325 +7,28[%] // -90[ppm]	[ppm]
Mg	Magnesium	987	933 -5,47[%] // -54[ppm]	613 -37,89[%] // -374[ppm]	629 -36,27[%] // -358[ppm]	[ppm]
P	Phosphorus	789,2	794 +0,6[%] // +4,8[ppm]	716,2 -9,25%] // -73[ppm]	719 -8,89[%] // -70,2[ppm]	[ppm]
Zn	Zinc	690,5	770 +11,51[%] // +79,5[ppm]	796,9 +15,4[%] // +106,4[ppm]	766,9 +11,06[%] // +76,4[ppm]	[ppm]
Cl	Chlorine	103	158,1 +53,49[%] // +55,1[ppm]	75,2 -26,99[%] // -27,8[ppm]	79,4 -22,91[%] // -23,6[ppm]	[ppm]
Si	Silicon	38,8	108 +178[%] // +69,2[ppm]	561 +1345,87[%] // +522,2[ppm]	603,5 +1455,41[%] // 564,7[ppm]	[ppm]
K	Potassium	26,7	29,2 +9,36[%] // +2,5[ppm]	11,9 -55,43[%] // -14,8[ppm]	17,2 -35,58%] // -9,5[ppm]	[ppm]
Mo	Molypden	1,6	7,1	8	7,4	[ppm]
Sr	Strontium	0,42	0,38	0,58	0,33	[ppm]
As	Arsenic	0,07	7,1	0	0,1	[ppm]
Tl	Thallium	0,06	0,06	0,07	<0,2	[ppm]
Br	Bromine	0	0,64	0,67	1,5	[ppm]
I	Iodine	<3,2	7	3,8	6	[ppm]
Al	Aluminum	<1,5	<1,6	<1,6	<1,6	[ppm]
Co	Cobalt	<0,1	<1	<1	<1	[ppm]
Mn	Manganese	<0,4	<0,4	<0,4	<0,4	[ppm]
Ag	Silver	<0,4	<0,4	<0,4	<0,4	[ppm]
Fe	Iron	<0,1	<1	<1	7,2	[ppm]
Cr	Chrome	<0,3	<0,4	<0,3	<0,3	[ppm]
Pb	Lead	<0,3	0,09	0,11	<0,3	[ppm]
Bi	Bismuth	<0,3	<0,3	<0,3	<0,3	[ppm]
Ba	Barium	<0,3	<0,3	<0,3	<0,3	[ppm]
Ni	Nickel	<0,1	<1	<1	<1	[ppm]
Zr	Zirconium	<0,2	<0,2	<0,2	<0,2	[ppm]

Hg	Mercury	<0,2	<0,2	<0,2	<0,2	[ppm]
Cu	Copper	<0,2	0,39	0,55	0,55	[ppm]
Sb	Antimony	<0,2	<1,6	<1,6	<1,6	[ppm]
Cd	Cadmium	<0,2	<0,2	<0,2	<0,2	[ppm]
Sn	Tin	<0,2	<1,1	<1,1	<1,1	[ppm]
Se	Selenium	<0,1	<0,1	<0,1	<0,1	[ppm]
W	Tungsten	<0,1	<0,1	<0,1	<0,1	[ppm]
V	Vanadium	<0,1	<0,1	<0,1	0	[ppm]
Ti	Titanium	<0,1	<0,1	<0,1	0	[ppm]

Source: author.

8 DROP TEST

It is an informative test used to determine the fitness of the EO. The presence of solid impurities, water, additive degradation and residual fuel in the EO are detected. The test was performed on a chromatographic filter and separation membrane. [10]

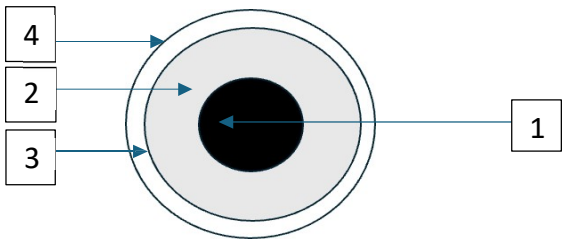

Fig. 20 Zone resemblance on separation membrane
Source: author.

8.1 Evaluating Part of Drop Test

- 1 - the inner black circle (No. 1) traps the heaviest impurities (of the type: hard sludge, soot, baked low and high heat sludge), also solid impurities coming from the external environment of the combustion engine.
- 2 - in the grey intermediate ring (No. 2) there can be impurities with lower weight than in the central ring, if there is a fine yellow colouring, we can conclude the state of degradation of EO addition.
- 3 - in this intermediate circle (No. 3), the lightest solid particles with the smallest mass are found, the yellow undercolouring on its border zone indicates the possible presence of additivation and water in the EO.
- 4 - on the last circle (No. 4), if a hilly structure called "peaky" is formed, we can say that there is residual fuel in the EO. [10]

Tab. 6 Evaluation table for particle density

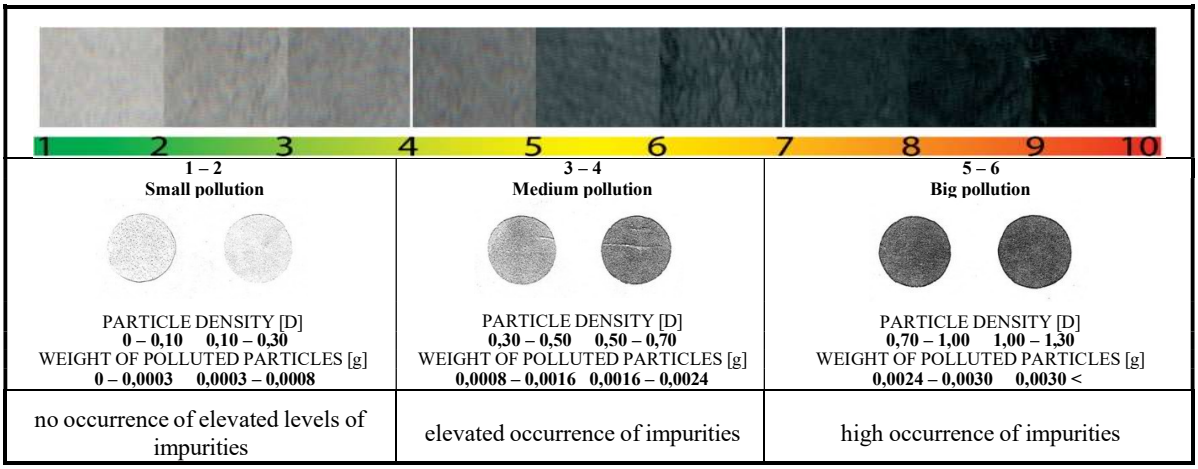

Source: author.

In the next section of the paper, the evaluation protocols of the EO samples are shown, in which the individual boundaries of the intermediate circles with different types of pollution are marked. The graphical visualization, shown on the right, is used to highlight transitions and boundaries during sample evaluation. [10]

The very small particles that characterize the first structure where the boundaries of the oil breakup at time Δt are located.

Medium sized particles, found at the transitions between the yellow and red markings on the liquefied sample.

Large particles deposited in the center of the liquefied sample.

8.2 Evaluation of Drop Text Protocol

Tab. 7 Evaluating protocol for drop test of referential sample of EO

Feature	Unit	Referential sample
Date of collection	[d.m.y]	23.02.2024
Date of measurement	[d.m.y]	23.02.2024
Milage of EO	[km]	0
Milage of vehicle	[km]	13 080
Right after dropping		**24 hours after the drop**

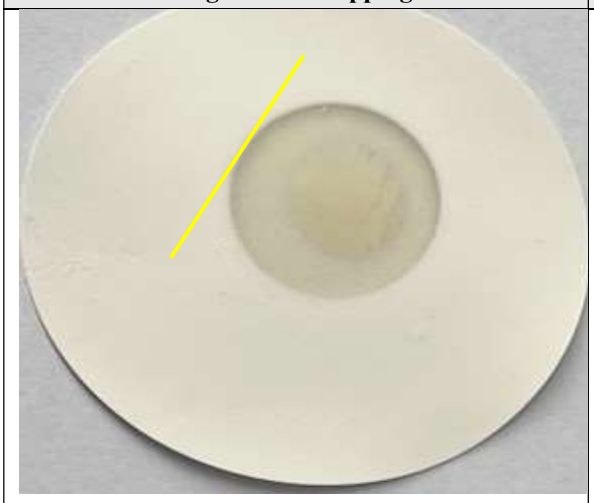

Fig. 21 Reference sample immediately after application on the separation membrane
Source: author.

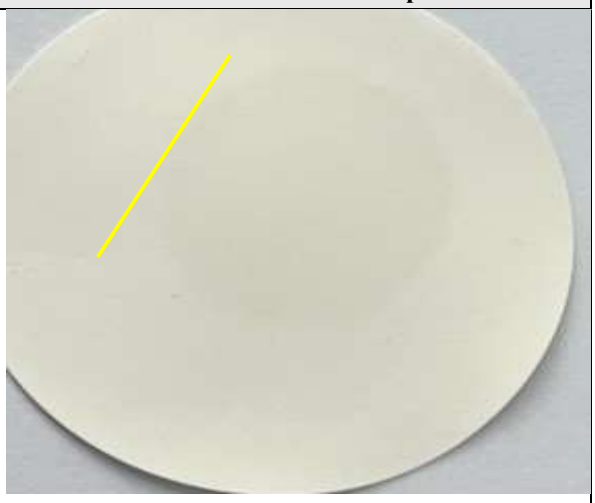

Fig. 22 Reference sample 24 h after application on the separation membrane
Source: author.

Evaluation of the reference pattern. on the separation membrane:
On the separation membrane (Fig. 22) the EO boundaries can be seen immediately after liquefaction and on the Fig. 23 side after 24 h. The scattering of the EO indicated by the yellow line can be seen. No dispersion-detergent particles are visible in the EO.

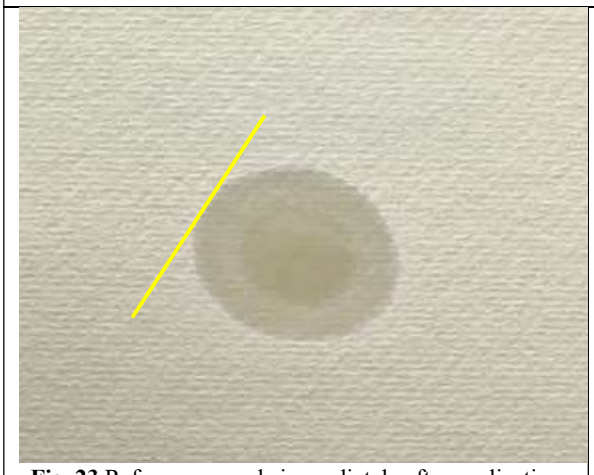

Fig. 23 Reference sample immediately after application to the chromatographic filter
Source: author.

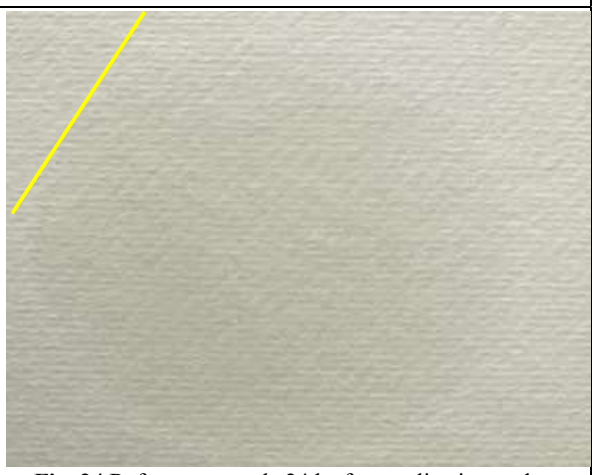

Fig. 24 Reference sample 24 h after application to the chromatographic filter
Source: author.

Evaluation of the reference pattern. on separation paper:
Comparing Fig. 20 and Fig. 21. The dispersion of oil on the chromatographic paper with absorbent structure can be seen. No dispersion-detergent particles are visible. The state of the addition is fine, the presence of water is not visible.

Source: author.

Tab. 8 Evaluation protocol for drop test of EO sample No. 1

Feature	Unit	Sample No.1
Date of collection	[d.m.y]	21.02.2024
Date of measurement	[d.m.y]	23.02.2024
Milage of EO	[km]	1 821
Milage of vehicle	[km]	14 901
Right after the drop		**24 hours after the drop**
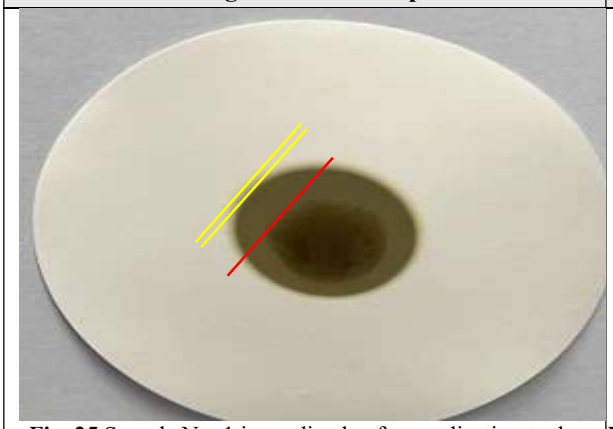		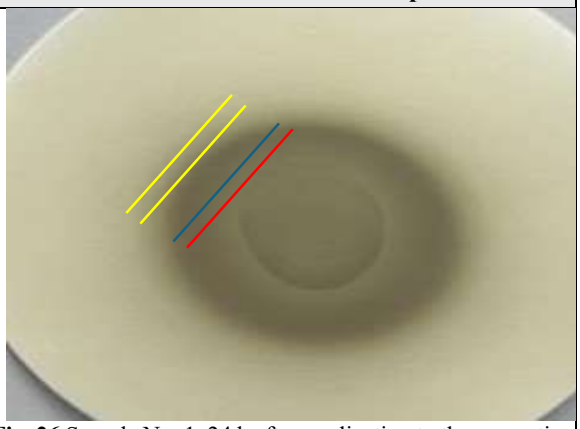
Fig. 25 Sample No. 1 immediately after application to the separation membrane Source: author.		**Fig. 26** Sample No. 1. 24 h after application to the separation membrane Source: author.
Evaluation of sample 1 on the separation membrane: Comparing the separation membranes, we see the separation of individual particles after 24 h. The density of the material is set to level 3 (in the range of 0.10 to 0.30).		
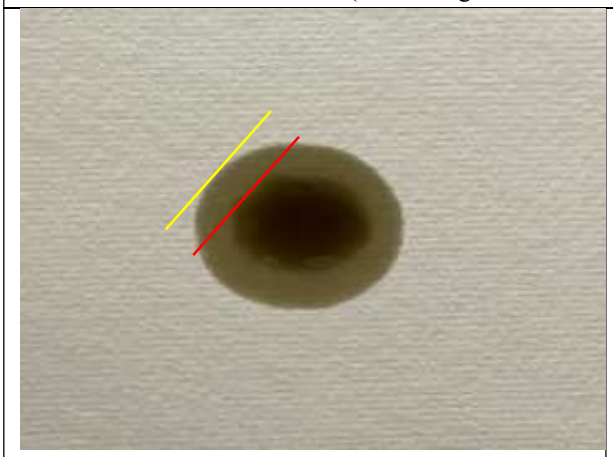		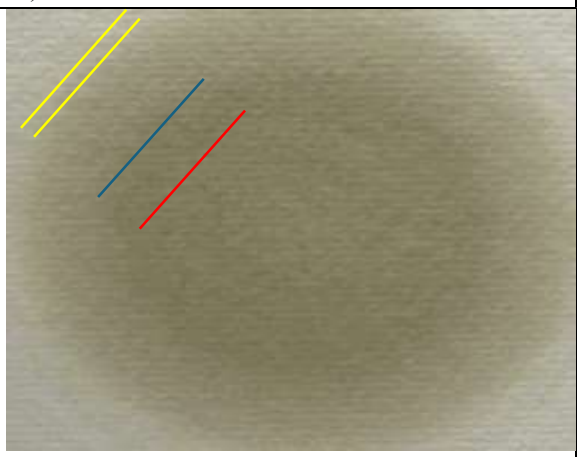
Fig. 27 Sample No. 1 immediately after application to the chromatographic filter Source: author.		**Fig. 28** Sample No. 1 24 h after application to the chromatographic filter Source: author.
Evaluation of the sample No. 1 on separation paper: When comparing the transitions of the chromatographic filter interrings immediately after application and after 24 h, it is visually visible. The heaviest particles have settled in the central part. The occurrence of water in the drop test is not visually visible. Based on particle density and drop test, EO sample #1 is passing.		

Source: author.

Tab. 9 Evaluation protocol for drop test of EO sample No. 2

Feature	Unit	Sample No. 2
Date of collection	[d.m.y]	22.05.2024
Date of measurement	[d.m.y]	12.07.2024
Milage of EO	[km]	1 986
Milage of vehicle	[km]	15 066
Right after the drop		**24 hours after drop**

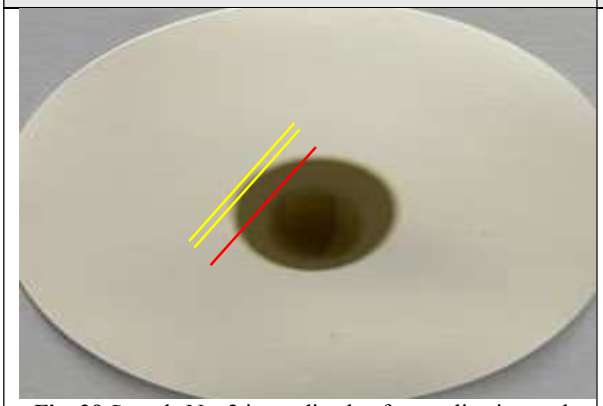

Fig. 29 Sample No. 2 immediately after application to the separation membrane
Source: author.

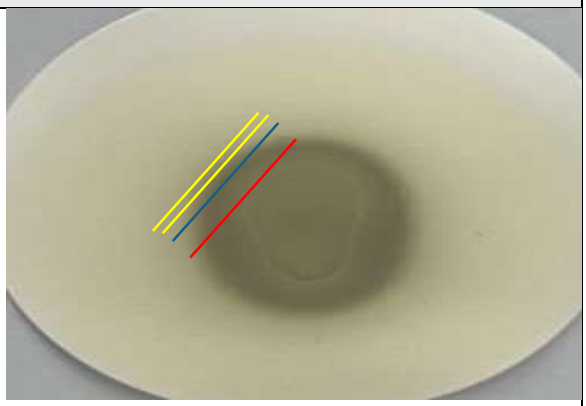

Fig. 30 Sample No. 2 immediately after application to the separation membrane
Source: author.

Evaluation of sample No. 2 on the separation membrane:
When comparing the separation membranes, the scattering of heavy particles is visible. These were formed in the EO by sintering in the combustion chamber and formed hard sludge, deposited in the centre of the separation membrane. The density of the dispersed particles is at level 4 (0.30 to 0.40).

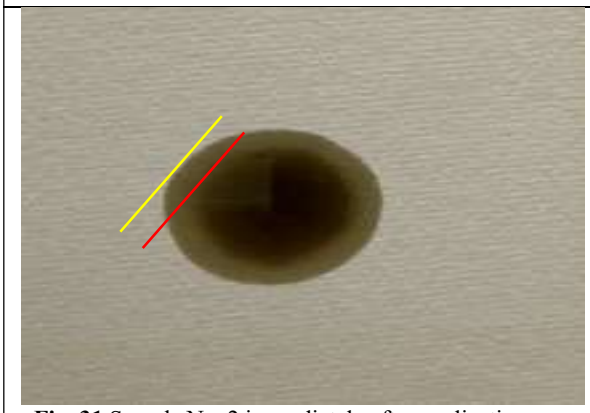

Fig. 31 Sample No. 2 immediately after application to the chromatographic filter
Source: author.

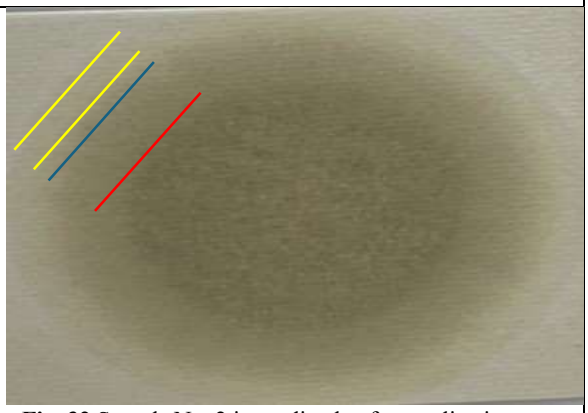

Fig. 32 Sample No. 2 immediately after application to the chromatographic filter
Source: author.

Evaluation of the sample No. 2 on separation paper:
Comparison of the chromatographic filters shows the dispersion of the EO into the individual intermediate rings, with the largest disperse-detergent particles deposited in the central part. The water content is not visible in the EO. The dark yellow colouration indicates the functionality of the additive component. The water and additive content can be detected more closely using the SpectroFluid instrument. EO sample No. 2 is satisfactory based on the drop test.

Source: author.

Tab. 10 Evaluation protocol for drop test of EO sample No. 3

Feature	Unit	Sample No. 3
Date of collection	[d.m.y]	04.09.2024
Date of measurement	[d.m.y]	06.09.2024
Milage of EO	[km]	4 546
Milage of vehicle	[km]	17 626
Right after the drop		**24 hours after the drop**

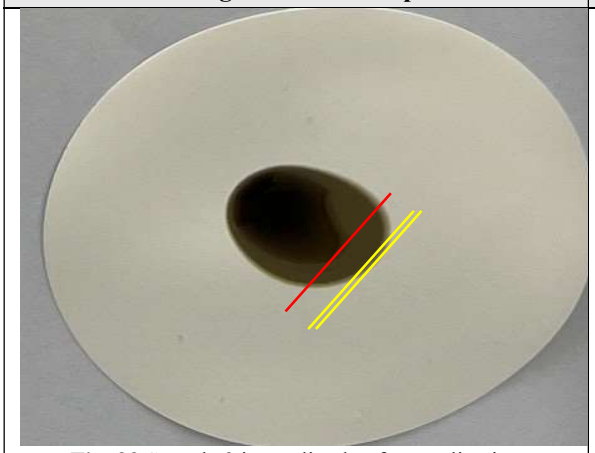

Fig. 33 Sample 3 immediately after application to the separation membrane
Source: author.

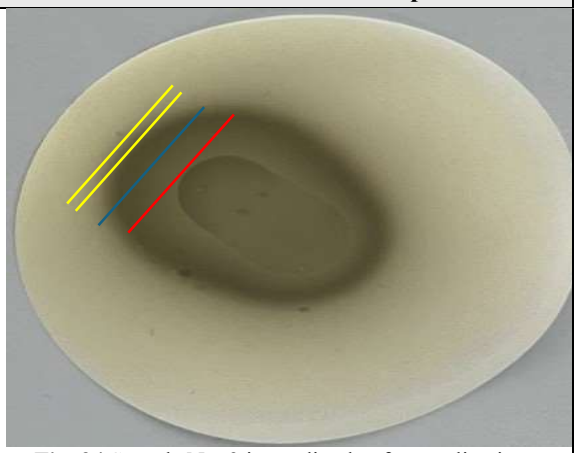

Fig. 34 Sample No. 3 immediately after application to the separation membrane
Source: author.

Evaluation of sample 3 on the separation membrane:
Sample No. 3 is significantly contaminated compared to the previous samples. The dark colouration of the MO indicates increased soot. The dispersed detergent particles are at 5-6.

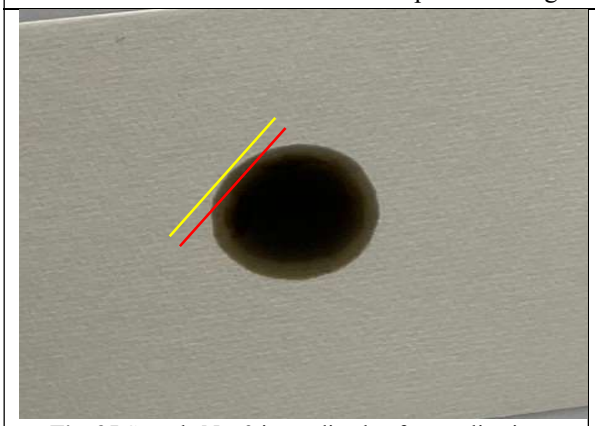

Fig. 35 Sample No. 3 immediately after application to the chromatographic filter
Source: author.

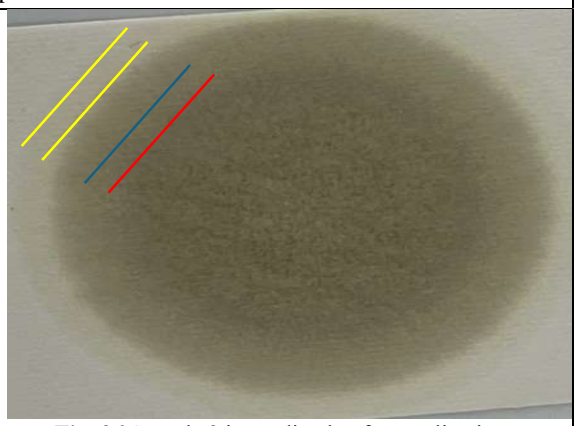

Fig. 36 Sample 3 immediately after application to the chromatographic filter
Source: author.

Evaluation of the sample No. 3 on separation paper:
Darkening of the EO is visible on the chromatographic filter. The dark yellow and greyish brown is caused by the EO burning through. The presence of water in the drop test is not visible. The additive content is within the standard based on the appearance of the intermediate rings and the yellow undertone of the chromatographic paper (filter). Sample EO No 3 is satisfactory on the basis of the drop test.

Source: author.

9 OVERALL CONCLUSION

All tests performed and values measured, including the indicative EO drop test, are satisfactory according to the evaluation parameters. In the operation of the vehicle and the subsequent replacement of the EO, the increased presence of silica 603,5 [ppm] requires more emphasis on the cleanliness of the intake tract or replacement with a higher quality air filter. Prolonged elevated silica levels may cause mechanical damage to combustion engine parts. The EO is further operable with the above caution.

References

[1] DAF, Acquire PSQL 2.1E Engine Oil approval for your product – DAF Trucks N.V. Available at: www.daf.com/en/suppliers/become-a-daf-supplier/acquire-psql21e-engine-oil-approval-for-your-product

[2] PILŠÁKOVÁ, E. and MARKO, M. *Vplyv degradačných činiteľov na kvalitu motorového oleja.* Diplomová práca. Liptovský Mikuláš: Akadémia ozbrojených síl generála Milana Rastislava Štefánika, 2012.

[3] KHONSARI, M. M. and BOOSER, E. R. *Applied Tribology: Bearing Design and Lubrication.* England: John Wiley & Sons, 2008. ISBN 9780470057117. Available at: https://doi.org/10.1002/9780470059456

[4] MARKO, M. *Aplikovaná chémia I. Vybrané aspekty tribotechniky, tribochémie a úvod do petrochémie.* Liptovský Mikuláš: Akadémia ozbrojených síl generála M. R. Štefánika, 2012. ISBN 978-80-8040-451-2.

[5] MARKO, M., DROPPA, P., ŠTIAVNICKÝ, M. a PAVLOV, Š. *BULLETIN č. 6. Vlastnosti a tribodiagnostika mazív v prevádzke motorových vozidiel.* Trenčín: Úrad logistického zabezpečenia Ozbrojených síl Slovenskej republiky, 2014. Available at: http://ak.aos.sk/images/dokumenty/e-knihy/MM-KTS/vatm.pdf

[6] LUKÁČ, M. a MARKO, M. *Vplyv prevádzky na degradáciu motorových olejov*. Diplomová práca. Liptovský Mikuláš: Akadémia ozbrojených síl generála M. R. Štefánika, 2013.

[7] *Paccar powetrain.* Available at: https://paccarpowertrain.com/products/epa-mx-13/

[8] SALGUEIRO, J. M., PERŠIN, G., HROVATIN, J., JURCIC, E. and VIŽINTIN, J. On-line detection of incipient trend changes in lubricant parameters. In *Industrial Lubrication and Tribology,* Vol. 67, No. 6, pp. 509-519. 2015. Available at: https://doi.org/10.29354/diag/169032

[9] SPECTRO AMETEK, Materials Analysis *Division. Spectro Cube ED-XRF spektrometer pre analýzu drahých kovov.* Available at: www.spectroaps.sk/wp-content/uploads/spectrocube_brochure_SK_lowpdf

[10] Súprava TRIBO-1, OTS VOP 083. Český Dub, 1983.

[11] MENEZES, P., L., INGOLE, S. P., NOSONOVSKY, M., KAILAS, S. V. and LOVELL, M. R. *Tribology for Scientists and Engineers: From Basic to Advances Concepts.* New York: Springer, 2013. ISBN 978-1-4614-1944-0. Available at: https://doi.org/10.1007/978-1-4614-1945-7_28

[12] LUKÁŠIK, P. Monitoring of engine oil degradation and possiblities of life predictions in combustion engine. In *Diagnostyka*, vol. 24, no. 3, 2023. Available at: https://doi.org/10.29354/diag/169032

[13] DROPPA, P., FILÍPEK, S. and ČORŇÁK, Š. The possibilities of using diagnostics and simulation methods to design and modernization of military technics. In *Transport Means 2016.* Proceedings of the 20th International Scientific Conference, Part 1. Kaunas (Lithuania): Kaunas University of Technology, 2016. pp. 156-160. ISSN 1822-296X.

[14] DROPPA, P., KALNA, P. and FILÍPEK, S. Application diagnostics methods for modernization vehicle IFV-2. In *International Conference on Military Technologies (ICMT),* 2015. Brno, Czech Republic: 2015. pp. 1-5. Available at: https://doi.org/10.1109/MILTECHS.2015.7153762

Bc. Adam **FULEK**
Armed Forces Academy of General M. R. Štefánik
Department of Mechanical Engineering
Demänová 393
031 01 Liptovsky Mikulas, Slovak Republic
E-mail: adam.fulek@aos.sk

Dipl. Eng. Vladimir **KADLUB**
Armed Forces Academy of General M R Štefánik
Department of Mechanical Engineering
Demänová 393
031 01 Liptovsky Mikulas, Slovak Republic
E-mail: vladimir.kadlub@aos.sk

Dipl. Eng. Miroslav **MARKO**, PhD.
Armed Forces Academy of General M. R. Štefánik
Department of Mechanical Engineering
Demänová 393
031 01 Liptovský Mikuláš, Slovak republic
E-mail: mikro_makro@pobox.sk
Miroslav.Marko@aos.sk

Adam FULEK was born in Ilava, Slovakia in 2001. He is student in Armed Forces Academy of General M. R. štefánik in Liptovský Mikuláš. His focus of study is propellants and materials at Department of Mechanical Engineering.

Vladimir KADLUB was born in Trstená, Slovakia in 1981. He received his M.Sc (Eng.) at the Armed Forces Academy in Liptovský Mikuláš in 2004. He started his dissertation studies in 2019. His research interests are focused on repairs and maintenance. He is currently working as an assistant professor at the Department of Mechanical Engineering, Armed Forces Academy of General M. R. Štefánik in Liptovský Mikuláš.

Miroslav MARKO was born on September 25, 1954 in Myjava, Slovakia. Between 1961 to 1970, he received his basic education in Stará Turá. Between 1970 to 1974, he received secondary education at the Grammar School in Nové Mesto and Váhom. From 1974 to 1978 VVŠ PV, university education in the field of „Operation and repair of the tank and automotive technology". From 1991 to 1993 VŠPe, additional pedagogical study, Faculty of Education Nitra. In 1997 House of Technology ZSVTS, Slovak Society for Tribology and Tribotechnics, postgraduate one-year study in Tribotechnik, Bratislava. From 1999 to 2004 Military Academy doctoral study – external. 91-06-9 Armament and ground forces technology, Liptovský Mikuláš in the field May 20, 2011.

SCIENCE & MILITARY - WRITER´S GUIDELINES

1. Scientific articles submitted for publishing have to be original, topical and never been published before.

2. Articles have to be written in English language and in accordance with ethical standards. For moredetails, please visit the website of the Science & Military Journal (https://www.aos.sk/en/article/science-military-ethical-standards).

3. Length of the article should not exceed 6 pages in defined format. Microsoft Word text editor must be used for writing. Articles must be written using Times New Roman, single line spacing and follow the following form: Title -12 point bold capital letters aligned to the center. Full author´s (co-author´s) name – 10 point normal letters aligned to the center. Abstract – 9 point normal letters, extent 3-5 lines. Keywords – 9 point normal letters. The article text – 10 point normal letters. Contact - full author´s (co-author´s) name, affiliation, e-mail – 9 point normal letters at the end of the article. The article text will be written in 2 columns format with a 75 mm column width and 10 mm empty space separating the columns. The first line of each paragraph must be shifted 5 mm to the right.

4. Upper and lower margins must be set to 25 mm, left and right margins to 20 mm. Select mirror margins and set binding margins to 10 mm. The distance between the header/footer and the page margin must be 12,5 mm, while different odd and even pages must be selected.

5. Photographs for publication must be in black-white (not in color) of excelent quality with good contrast.

6. Equations in the text are also to be written using the equation editor. (Equation must be typed in Microsoft Equation, which is an integral part of Microsoft text editor.) They must be numbered. Numbers are to be enclosed in parentheses and aligned to the right margin of a column.

7. Figures, graphs and tables must be included in the text and numbered and must contain description. Figures must be identified as Fig. 1 followed gradually by the figure description. Graphs must be identified as Graph 1 followed by the graph description. Tables must be identified as Tab. 1, followed by the table description.

8. References must be fully and accurately documented (according to ISO 690). References should be quoted in the text in square brackets and listed in the order they have appear in the text.

9. The specimen article that can be found on the web-site: https://www.aos.sk/en/article/science-military-for-authors can be used as an example of the correct format.

10. The editorial board will consider submitted articles in the next scheduled meeting. If it decides to include the article in the next issue it submits the manuscript to the editors for the peer review. The final version (before printing) will be sent to the author for the final revision. The authors are fully responsible for the level of language.

11. Contributions in A4 format edited according to the specimen article should be submitted in one hard copy and also in electronic form to the Editorial board.

12. The deadlines for the delivery of the articles in calendar year are: March 1 and September 1.

SCIENCE & MILITARY

No 1 | Volume 20 | 2025

Content

ISSN 1336 – 8885 (print)
ISSN 2453 – 7632 (online)